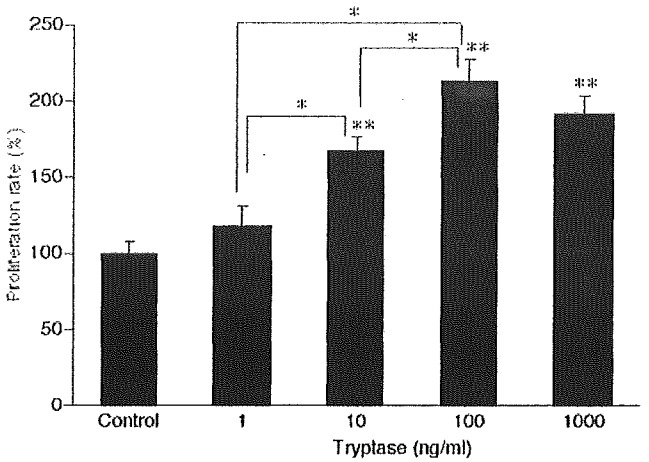

FIGURE 1. Proliferation of cultured conjunctival fibroblasts incubated with various concentration of tryptase. Tryptase increased the proliferation of conjunctival fibroblasts in a statistically significant and dose-dependent manner (*$P < 0.05$; **$P < 0.05$ compare to control). No further increase above 100 ng/mL was observed. The data are representative of experiments using fibroblasts from three different donors.

performed in triplicate, using fibroblasts from three different donors. Tryptase produced a statistically significant increase in conjunctival fibroblast proliferation in a dose-dependent manner, with maximum proliferation observed at a dose of 100 ng/mL ($P < 0.05$; Fig. 1).

Existence of PAR-2 on Conjunctival Fibroblasts

We investigated the existence of mRNA for the known tryptase receptor, PAR-2, in human conjunctival fibroblasts using RT-PCR. Primary cultured fibroblasts from three different donors were used for the assay. PAR-2 mRNA was detected in all specimens from three different donors (Fig. 2A).

Next, we examined the existence of PAR-2 protein on human conjunctival fibroblasts using Western blot analysis. Primary cultured fibroblasts from three different donors were used for the assay. PAR-2 protein was detected in the specimens from all three different donors (Fig. 2B).

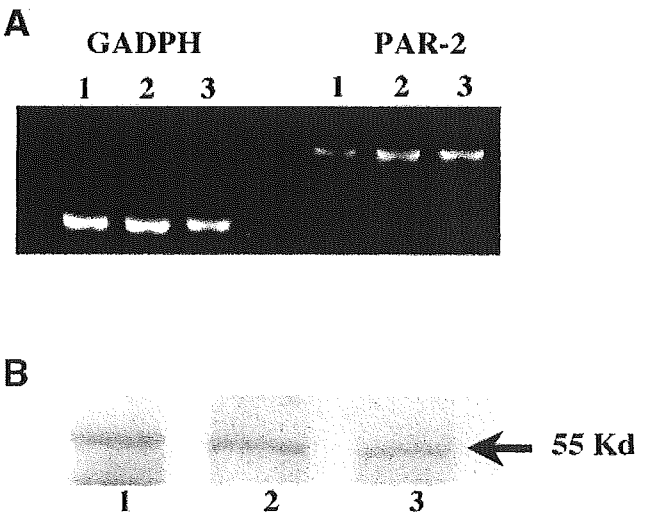

FIGURE 2. Existence of PAR-2 mRNA and protein on human conjunctival fibroblasts. (A) RT-PCR analysis shows PAR-2 mRNA expression in cultured conjunctival fibroblasts. (B) Western blot analysis shows the presence of a 55-kDa protein (PAR-2) in cultured conjunctival fibroblasts.

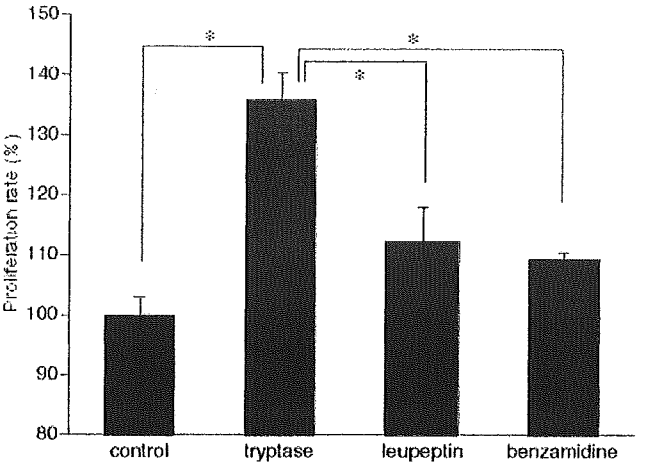

FIGURE 3. Effects of the protease inhibitors leupeptin and benzamidine on tryptase-induced conjunctival fibroblast proliferation. Both leupeptin (10^{-4} M) and benzamidine (10^{-4} M) significantly inhibited 100 ng/mL of tryptase-induced conjunctival fibroblast proliferation (*$P < 0.05$).

Inhibition of Cell Proliferation by Tryptase Inhibitors

We next examined the inhibition of tryptase inhibitors on the proliferative activity of tryptase-stimulated conjunctival fibroblasts. Leupeptin and benzamidine are known to inhibit the catalytic activity of tryptase. After conjunctival fibroblasts were cultured in 96-well culture plates (5000 cells per well) for 24 hours in DMEM/F12 supplemented with FCS, the medium was replaced with serum-free DMEM/F12 containing 100 ng/mL of tryptase with or without inhibitors. The culture medium was preincubated with 100 ng/mL of tryptase, or 100 ng/mL of tryptase and 10^{-4} M of each inhibitor at 37.0°C for 1 hour before use. Both leupeptin and benzamidine significantly in-

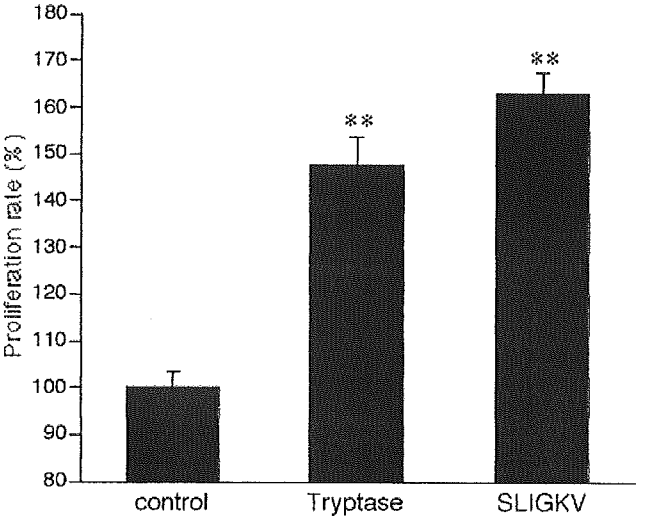

FIGURE 4. Effect of the PAR-2 agonist SLIGKV on conjunctival fibroblast proliferation. The PAR-2 agonist SLIGKV (10^{-4} M) mimicked 100 ng/mL of tryptase's effect and significantly increased the proliferation of conjunctival fibroblasts (*$P < 0.05$).

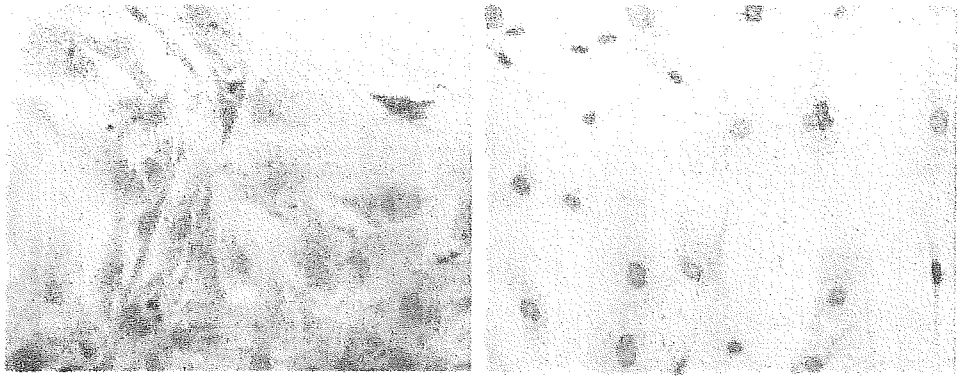

FIGURE 5. Immunoreactivity of PAR-2 receptor protein in cultured conjunctival fibroblasts. *Left*: immunohistochemistry shows that PAR-2 immunoreactivity was observed in cultured conjunctival fibroblasts. *Right*: isotype control.

hibited effect of tryptase on the proliferative activity of the cells (Fig. 3; $P < 0.05$).

The Effect of PAR-2 Agonist on Conjunctival Fibroblast Proliferation

Human PAR-2 is known to be activated by a synthetic peptide, SLIGKV. SLIGKV is designed based on the amino acid sequence of the tethered ligand, which directly binds to the body of PAR-2 without cleaving the N-terminal peptide, acting as an agonist for PAR-2.[14,15] SLIGKV mimicked the effect of tryptase (100 ng/mL of dose) and significantly increased the proliferative activity of cultured conjunctival fibroblasts (Fig. 4; $P < 0.05$).

Immunoreactivity of PAR-2 in Conjunctival Fibroblasts

We assessed the existence of PAR-2 receptor protein in conjunctival fibroblasts. In cultured conjunctival fibroblasts, PAR-2 immunoreactivity was observed except cell nucleus (Fig. 5). Because the anti-PAR-2 antibody, SAM-11 binds to the amino acid sequence 37-50, which is contained in the amino terminal of exodomain of human PAR-2, we strongly suspected that this staining pattern reflected PAR-2 localization on the cell membrane.

In the surgically excised papillae from patients with VKC, there were many tryptase-positive cells within the inflammatory cell infiltration site, whereas conjunctival tissues from normal volunteers contained no tryptase-positive cells. In both surgically excised papillae from patients with vernal keratoconjunctivitis and conjunctival tissue from normal control subjects, fibroblast-like cells with a flattened appearance were positively stained by the PAR-2 antibody (Fig. 6).

DISCUSSION

In this study, we showed that tryptase upregulated the proliferative activity of cultured conjunctival fibroblasts and that this stimulation was mediated by the known tryptase receptor, PAR-2. To the best of our knowledge, this is the first report indicating that conjunctival fibroblasts, in addition to fibroblasts derived from lung or dermal tissue, express PAR-2 and proliferate after stimulation with tryptase.

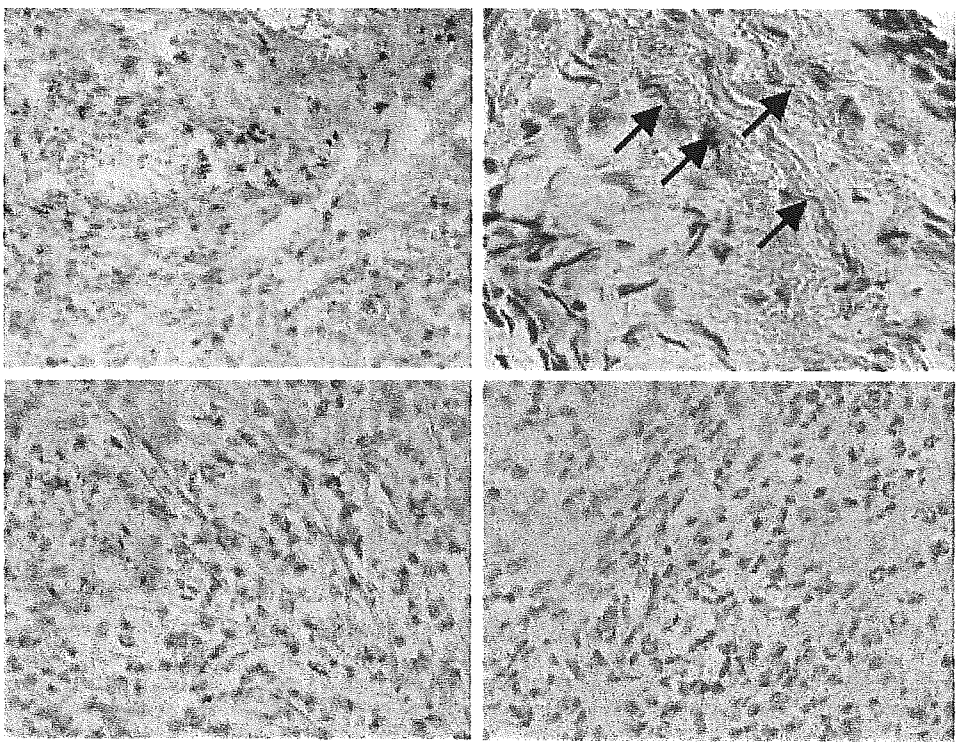

FIGURE 6. Immunoreactivity of human mast cell tryptase and PAR-2 receptor protein in conjunctival fibroblasts from surgically excised papillae. *Top left*: immunohistochemistry shows tryptase immunoreactive cells are observed within the area with inflammatory cell infiltration in the papillae from VKC specimens. *Top right*: PAR-2 immunoreactive stromal fibroblasts (*arrows*) are observed in conjunctival tissues from normal volunteers. *Bottom left*: PAR-2 immunoreactivity is seen in spindle-shaped cells, thought to be fibroblasts, in surgically excised papillary specimens from patients with VKC. *Bottom right*: isotype control shows no immunoreaction.

Tryptase is mainly released by mast cells. Mast cells activated by IgE binding to FcεRI play a critical role in the early phase of allergic inflammation, releasing preformed mediators like histamine, chymase, cathepsin-G, and mast-cell-specific carboxypeptidase A. Human mast cells produce α and β forms of tryptase. α-Tryptase is constitutively produced, while β-tryptase is stored in the secretory granules and released by exocytosis.[11] Our current results revealed that β-tryptase upregulated fibroblast proliferation, indicating that mast cells can affect the mitogenic acceleration of fibroblasts, when activated.

Like fibroblasts derived from lung or skin, conjunctival fibroblasts are known to produce various factors and affect other type of cells, including leukocytes. Previous investigation reported that conjunctival fibroblasts secreted Th-2 cytokines,[19] eotaxin,[20] procollagen type I and III,[21–23] MMPs,[23] and VEGF.[24] Solomon et al.[25] reported that conjunctival fibroblasts enhanced the survival and functional activity of eosinophils through IL-3, IL-5, and granulocyte-macrophage colony-stimulating factor. Leonardi et al.[26] reported that histamine, which is accumulated in preformed granules in mast cells as well as tryptase, increases the proliferative and productive activity of conjunctival fibroblasts in patients with VKC. These facts may indicate a hypothesis that mast cells activate residential conjunctival stromal cells through the degranulation of preformed mediators, resulting in massive leukocyte infiltration and excess fibrovascular proliferation, causing giant papillary formation. Thus, mast cells may affect tissue remodeling[27] in allergic conjunctiva.

PAR-2 is known to be the sole receptor of tryptase. The current results show that the proliferative activity upregulated by tryptase was almost totally inhibited by leupeptin and benzamidine and that the PAR-2 antagonist peptide SLIGKV completely mimicked the effect of tryptase. These findings suggest that the local administration of a PAR-2-blocking peptide may effectively inhibit fibroblast proliferation in conjunctival tissue in vivo. We also demonstrated the existence of PAR-2 mRNA and protein on cultured conjunctival fibroblasts derived from normal volunteers, as well as on stromal fibroblasts in giant papillae from patients with VKC. We speculate that under allergic conditions, when Th-2 cytokines or proinflammatory factors are abundant, PAR-2 expression on conjunctival stromal cells may be upregulated. A quantitative assessment of PAR-2 expression on conjunctival fibroblasts would provide interesting data.

In conclusion, tryptase upregulates conjunctival fibroblast proliferation, and this effect appeared to be mediated via the PAR-2 receptor. Mast cells may play an important role in giant papillary formation during late-phase allergic conjunctivitis by means of releasing tryptase. Inhibitors of tryptase or peptides that block PAR-2 on the surfaces of fibroblasts may offer therapeutic benefits by selectively preventing the activation of fibroblasts and consequently the formation of giant papillae, in patients with allergic conjunctivitis. Further investigations are required in this field.

Acknowledgments

The authors thank Ayako Igarashi and Akiko Kujira for technical help.

References

1. Anderson DF, MacLeod JD, Baddeley SM, et al. Seasonal allergic conjunctivitis is accompanied by increased mast cell numbers in the absence of leucocyte infiltration. *Clin Exp Allergy*. 1997;27:1060–1066.
2. Baddeley SM, Bacon AS, McGill JI, Lightman SL, Holgate ST, Roche WR. Mast cell distribution and neutral protease expression in acute and chronic allergic conjunctivitis. *Clin Exp Allergy*. 1995;25:41–50.
3. Morgan SJ, Williams JH, Walls AF, Holgate ST. Mast cell hyperplasia in atopic keratoconjunctivitis: an immunohistochemical study. *Eye*. 1991;5:729–735.
4. Irani AM, Butrus SI, Tabbara KF, Schwartz LB. Human conjunctival mast cells: distribution of MCT and MCTC in vernal conjunctivitis and giant papillary conjunctivitis. *J Allergy Clin Immunol*. 1990;86:34–40.
5. Yao L, Baltatzis S, Zafirakis P, et al. Human mast cell subtypes in conjunctiva of patients with atopic keratoconjunctivitis, ocular cicatricial pemphigoid and Stevens-Johnson syndrome. *Ocul Immunol Inflamm*. 2003;11:211–222.
6. Tabbara KF. Tear tryptase in vernal keratoconjunctivitis. *Arch Ophthalmol*. 2001;119:338–342.
7. Bacon AS, Ahluwalia P, Irani AM, et al. Tear and conjunctival changes during the allergen-induced early- and late-phase responses. *J Allergy Clin Immunology*. 2000;106:948–954.
8. Margrini L, Bonini S, Centofanti M, Schiavone M, Bonini S. Tear tryptase levels and allergic conjunctivitis. *Allergy*. 1996;51:577–581.
9. Butrus SI, Ochsner KI, Abelson MB, Schwarts JB. The level of tryptase in human tears: an indicator of activation of conjunctival mast cells. *Ophthalmology*. 1990;97:1678–1683.
10. Anderson DF, Zhang S, Bradding P, McGill JI, Holgate ST, Roche WR. The relative contribution of mast cell subsets to conjunctival TH2-like cytokines. *Invest Ophthalmol Vis Sci*. 2001;42:995–1001.
11. Bingham CO, Austen KF. Mast-cell response in the development of asthma. *J Allergy Clin Immunol*. 2000;105:S527–S534.
12. Nystedt S, Emilsson K, Wahlestedt C, Sundelin J. Molecular cloning of a potential proteinase activated receptor. *Proc Natl Acad Sci USA*. 1994;91:9208–9212.
13. Kawabata A, Kuroda R. Protease-activated receptor (PAR), a novel family of G protein-coupled seven trans-membrane domain receptors: activation mechanisms and physiological roles. *Jpn J Pharmacol*. 2000;82:171–174.
14. Kawabata A. Physiological functions of protease-activated receptor-2. *Folia Pharmacol Jpn*. 2003;121:411–420.
15. Kawabata A. PAR-2: structure, function and relevance to human diseases of the gastric mucosa. *Expert Rev Mol Med*. 2002;16:1–17.
16. Akers IA, Parsons M, Hill MR, et al. Mast cell tryptase stimulates human lung fibroblast proliferation via protease-activated receptor-2. *Am J Physiol*. 2000;278:L193–L201.
17. Frungieri MB, Weidinger S, Meineke V, Köhn FM, Mayerhofer A. Proliferative action of mast-cell tryptase is mediated by PAR-2, COX2, prostaglandins, and PPAR-γ: possible relevance to human fibrotic disorders. *Proc Natl Acad Sci USA*. 2002;99:15072–15077.
18. Cubitt CL, Tang Q, Monteiro CA, Lausch RN, Oakes JE. IL-8 gene expression in cultures of human corneal epithelial cells and keratocytes. *Invest Ophthalmol Vis Sci*. 1993;34:3199–3206.
19. Leonardi A, DeFranchis G, De Paoli M, Fregona I, Plebani M, Secchi A. Histamine-induced cytokine production and ICAM-1 expression in human conjunctival fibroblasts. *Curr Eye Res*. 2002;25:189–196.
20. Leonardi A, Jose PJ, Zhan H, Calder VL. Tear and mucus eotaxin-1 and eotaxin-2 in allergic keratoconjunctivitis. *Ophthalmology*. 2003;110:487–492.
21. Fujitsu Y, Fukuda K, Kumagai N, Nishida T. IL-4-induced cell proliferation and production of extracellular matrix proteins in human conjunctival fibroblasts. *Exp Eye Res*. 2003;76:107–114.
22. Leonardi A, DeFranchis G, Fregona IA, Violato D, Plebani M, Secchi AG. Effects of cyclosporin A on human conjunctival fibroblasts. *Arch Ophthalmol*. 2001;119:1512–1517.
23. Leonardi A, Cortivo R, Fregona I, Plebani M, Secchi AG, Abatangelo G. Effects of Th2 cytokines on expression of collagen, MMP-1, and TIMP-1 in conjunctival fibroblasts. *Invest Ophthalmol Vis Sci*. 2003;44:183–189.
24. Asano-Kato N, Fukagawa K, Okada N, et al. TGF-beta, IL-1beta, and Th2 cytokines stimulate vascular endothelial growth factor production from conjunctival fibroblasts. *Exp Eye Res*. 2005;80:555–560.
25. Solomon A, Shmilowich R, Shasha D, et al. Conjunctival fibroblasts enhance the survival and functional activity of peripheral blood eosinophils in vitro. *Invest Ophthalmol Vis Sci*. 2000;41:1038–1044.
26. Leonardi A, Radice M, Fregona IA, Plebani M, Abatangelo G, Secchi AG. Histamine effects on conjunctival fibroblasts from patients with vernal conjunctivitis. *Exp Eye Res*. 1999;68:739–746.
27. Vignola AM, Mirabella F, Costanzo G, et al. Airway remodeling in asthma. *Chest*. 2003;123(suppl 3):417S–422S.

The Implications of the Upregulation of ICAM-1/VCAM-1 Expression of Corneal Fibroblasts on the Pathogenesis of Allergic Keratopathy

Naoko Okada,[1,2] *Kazumi Fukagawa,*[1,2] *Yoji Takano,*[1,3] *Murat Dogru,*[1] *Kazuo Tsubota,*[1] *Hiroshi Fujishima,*[1] *Kenji Matsumoto,*[2] *Toshiharu Nakajima,*[2] *and Hirohisa Saito*[2]

Objective. The present study investigated the expression of ICAM-1 and VCAM-1 on fibroblasts with interleukin (IL)-4 and/or tumor necrosis factor (TNF)-α stimulation and assessed the effect of eosinophil adhesion on fibroblast viability.

Methods. Primary cultured human corneal fibroblasts were incubated with IL-4, TNF-α, or their combination for 24 hours. Expression of ICAM-1 and VCAM-1 was examined by real-time quantitative PCR and flow cytometric analysis. Purified eosinophils were cocultured with activated fibroblasts, and the number of eosinophils adhered to fibroblasts and the number of damaged fibroblasts were counted using microscopy. In a separate trial, conjunctival and corneal impression cytology was performed on patients with atopic keratoconjunctivitis and corneal ulcers (eight eyes) to assess the status of the ocular surface epithelium and the presence of inflammatory cell infiltrates.

Results. Real-time quantitative PCR and flow cytometric analysis revealed that both mRNA and protein of VCAM-1 and ICAM-1 were upregulated by IL-4 and TNF-α. IL-5-primed eosinophils adhered to the corneal fibroblasts treated with IL-4 and TNF-α, and the fibroblasts were damaged by eosinophil adherence. Anti-ICAM-1 antibody and anti-VCAM-1 antibody inhibited the eosinophil adherence to fibroblasts and the fibroblast damage. Impression cytology revealed extensive infiltration of neutrophil and eosinophils among isolated ocular surface epithelial cells with advanced squamous metaplasia.

Conclusions. Corneal fibroblasts expressed ICAM-1 and VCAM-1 when activated with IL-4 and TNF-α. Eosinophils can adhere to the activated fibroblasts and can induce subsequent fibroblast damage through these adhesion molecules. Eosinophil adhesion to fibroblasts may possibly contribute to the pathogenesis of severe persistent allergic corneal ulcers. (*Invest Ophthalmol Vis Sci.* 2005;46:4512–4518) DOI:10.1167/iovs.04-1494

Eosinophils are thought to exacerbate the late-phase inflammatory response in immediate-type allergic reactions by releasing leukotrienes and highly cytotoxic proteins, such as major basic protein (MBP) and eosinophilic cationic protein (ECP).[1] These proteins may cause a variety of corneal disorders, including superficial punctate keratopathy and corneal ulcer in vernal keratoconjunctivitis (VKC) and atopic keratoconjunctivitis (AKC).[2–5] The presence of eosinophils and the deposition of ECP have already been observed in conjunctival tissues and in tears of patients with AKC and VKC.[6–10] MBP deposits were also observed in allergic corneal ulcers.[11] Purified MBP and ECP reduced corneal epithelial cell viability and caused morphologic changes in vitro.[12] These findings strongly suggest that eosinophils play an important role in the pathogenesis of allergic corneal ulcer. However, the precise mechanisms by which eosinophils damage the corneal tissue remain unclear.

Allergic reactions in the conjunctiva induce the release from inflammatory cells of various types of cytokines, including proinflammatory cytokines and helper type 2 T-cell (Th2) cytokines. Levels of interleukin (IL)-4 and tumor necrosis factor (TNF)-α in the tears of patients with allergies were found to be significantly higher than in healthy subjects.[13,14] These cytokines are known to modulate various functions of fibroblasts, such as eotaxin production and adhesion molecule expression.[15,16] Eotaxin is known to induce further recruitment of eosinophils.[17] On the other hand, adhesion molecules are thought to play an important role in the binding of eosinophils, through which eosinophils are believed to be stimulated further to release inflammatory mediators.[18,19]

Recently, it has been found that CD11/18-dependent adhesion is a critical step in human eosinophil degranulation.[20,21] Eosinophils express all four members of the CD18 (β2) leukocyte integrin family, CD11a to -d, which allow them to bind to their ligands, ICAM-1 to -3.[22–27] Eosinophils also express CD49d/CD29, which bind to the ligand VCAM-1.[28] In human lung fibroblasts, IL-4– and TNF-α–dependent expression of ICAM-1 and VCAM-1 and the influence of eosinophil-fibroblast adhesion on eosinophil degranulation have been reported.[29] However, it is still unclear how the eosinophil-fibroblast interactions influence allergic corneal inflammation, especially the course of corneal ulcer formation. We believed that actual adhesion of eosinophils to corneal fibroblasts through ICAM-1 and/or VCAM-1 might induce subsequent activation and might contribute to the evolution of persistent allergic corneal ulcers. Therefore, we initially looked into the changes of expression of ICAM-1 and VCAM-1 on stimulating corneal fibroblast cultures by IL-4 and TNF-α by employing flow cytometry and real-time PCR. We also cocultured corneal fibroblasts with eosinophils to assess the adhesion between the two cell types. We then investigated the timewise cell damage on corneal fibroblasts after eosinophil binding, as well as the effects of anti-ICAM-1 and anti-VCAM-1 applications on eosinophil adhesion and eosinophil-induced damage to the corneal fibroblasts. In addition, we performed conjunctival and corneal impression cytology on patients with AKC and corneal ulcers to evaluate the status of the ocular surface epithelium and the presence of eosinophils in the inflammatory response, if any.

From the [1]Department of Ophthalmology, Keio University, Tokyo, Japan; the [2]Department of Allergy and Immunology, National Research Institute for Child Health and Development, Tokyo, Japan; and the [3]Department of Ophthalmology, Kawasaki Hospital, Kanagawa, Japan.

Presented at the 26th Japan Cornea Congress, Osaka, Japan, February 2002; presented in part at the annual meeting of the Association for Research in Vision and Ophthalmology, Fort Lauderdale, Florida, May 2002.

Submitted for publication December 18, 2004; revised May 18 and August 12, 2005; accepted October 14, 2005.

Disclosure: **N. Okada**, None; **K. Fukagawa**, None; **Y. Takano**, None; **M. Dogru**, None; **K. Tsubota**, None; **H. Fujishima**, None; **K. Matsumoto**, None; **T. Nakajima**, None; **H. Saito**, None

The publication costs of this article were defrayed in part by page charge payment. This article must therefore be marked "*advertisement*" in accordance with 18 U.S.C. §1734 solely to indicate this fact.

Corresponding author: Naoko Okada, Department of Ophthalmology, Keio University School of Medicine, 35 Shinanomachi, Shinjukuku, Tokyo 160-8582, Japan; mi051006@sc.itc.keio.ac.jp.

Investigative Ophthalmology & Visual Science, December 2005, Vol. 46, No. 12

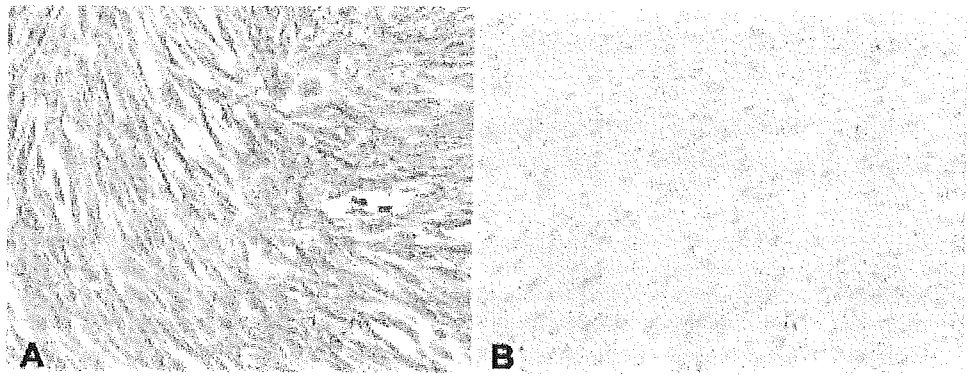

FIGURE 1. Immunohistochemistry staining of corneal fibroblasts by antivimentin antibodies. (A) Image shows diffuse positive staining with antivimentin antibodies (rabbit polyclonal, 1:2000 dilution; Lab Vision Corporation, Fremont, CA) and a lack of impurities from the presence of any other cell types in the slide chamber (magnification 200×). (B) Image shows the absence of staining in the negative control specimen (magnification 200×).

MATERIALS AND METHODS

Primary Cell Cultures

Three human corneas were obtained from the American Eye Bank Association. Briefly, after the center of each cornea was punched out for transplantation, the remaining rim of tissue was used to prepare corneal fibroblasts. The human tissue was used in strict accordance with the tenets of the Declaration of Helsinki. Corneal tissue was cut into pieces and then placed on collagen-coated 35-mm culture dishes (Iwaki, Tokyo, Japan). Corneal fibroblasts were isolated from corneal tissue explants and cultured with fibroblast culture medium composed of Dulbecco's modified Eagle's medium and Ham's nutrient mixture F-12 (DMEM-F12; Gibco-BRL, Grand Island, NY), supplemented with 10% fetal calf serum (FCS; Gibco), 100 IU/mL penicillin, and 100 μg/mL streptomycin (all supplied by Invitrogen-Gibco Life Technologies, Paisley, UK) at 37°C with 5% (vol/vol) CO_2 in air. Cultures of passages 3 and 6 were used in the present study. The purity of the cell cultures was assessed on the basis of both the distinctive morphology of corneal fibroblasts and their reactivity with antibodies to vimentin and isotype control in immunohistochemistry analysis. No contamination by corneal epithelial cells was detected (Fig. 1).

Isolation of Human Eosinophils

Human granulocytes were isolated from heparin-anticoagulated venous blood of atopic volunteers. The granulocytes underwent Percoll density gradient centrifugation (490g) at room temperature, and CD16-positive cells were removed using immunomagnetic beads (Miltenyi Biotec GmbH, BergischGladbach, Germany) as previously described.[30] Eosinophil purity of cytocentrifuge preparations was determined by staining (Diff-Quick; American Scientific Products, McGraw Park, IL) and was confirmed to be greater than 98%.

Quantitative Real-Time PCR

We confirmed whether ICAM-1 and VCAM-1 mRNA expressions were correlated with the concentrations of IL-4 and TNF-α by performing quantitative measurements of ICAM-1 and VCAM-1 mRNA with real-time PCR. The primary human corneal fibroblasts from three different donors were cultured for 24 hours with various cytokine concentrations, after which total RNA was extracted. RNA was extracted from corneal fibroblasts cultured in the presence or absence of 0.3 to 30 ng/mL IL-4 and TNF-α for 24 hours. A commercially available sequence detection system (ABI PRISM 7700; Applied Biosystems, Warrington, UK) and gene expression assay mixes (TaqMan Universal PCR Master Mix and Assay-on-Demand Gene Expression Assay Mix; Applied Biosystems) were used for real-time quantitative PCR to measure for ICAM-1, VCAM-1, and GAPDH. The thermal profile consisted of 50°C for 2 minutes and 95°C for 10 minutes, followed by 40 cycles of 94°C for 15 seconds and 60°C for 1 minute. Results were analyzed by the comparative cycle threshold method.[31,32]

Flow Cytometry Analysis

To examine the ICAM-1 and VCAM-1 protein expression on the cell surface of cultured fibroblasts, flow cytometric analysis was performed 24 hours after cytokine stimulation. IL-4– and/or TNF-α–stimulated corneal fibroblasts were gently removed from the six well-culture dishes with cell dissociation buffer (Gibco-BRL), washed, and diluted in PBS containing 1% BSA and 0.1% NaN_3. Cells were stained by monoclonal antibodies against mouse IgG_1 (Sigma, St. Louis, MO), ICAM-1 (84H10; Immunotech, Marseille, France) or VCAM-1 (1G11; Immunotech), respectively, and analyzed by flow cytometry (FACScan, Becton Dickinson, Franklin Lane, NJ) and analysis software (CellQuest; Becton Dickinson, Mountain View, CA).

Eosinophil-Fibroblast Adhesion Assay

To determine the functional significance of ICAM-1 and VCAM-1 expression on cultured fibroblasts, in vitro eosinophil adhesion experiments were performed. Corneal fibroblasts from three different donors were cultured in 96-well culture plates (Becton-Dickinson Labware, Lincoln Park, NJ) for 48 hours After starvation for 24 hours, the cells were stimulated with IL-4 (1–100 ng/mL) and/or TNF-α (1–100 ng/mL)

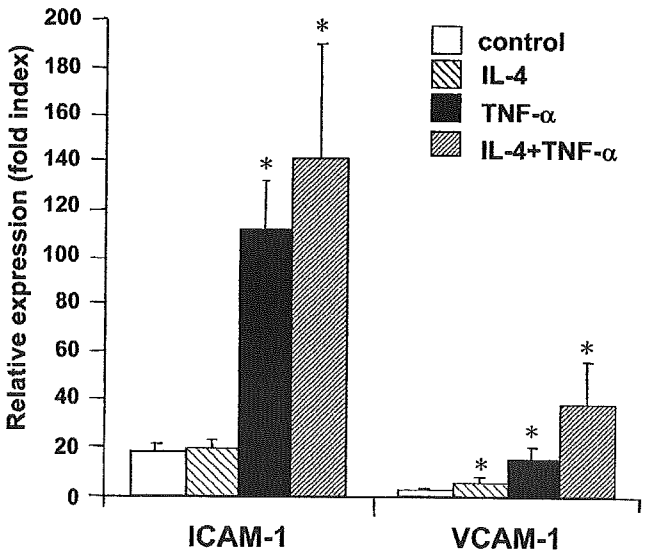

FIGURE 2. Relative expression of mRNA encoding ICAM-1 and VCAM-1 on corneal fibroblasts compared to controls. Corneal fibroblasts were incubated with IL-4 (0.3–30 ng/mL), TNF-α (0.3–30 ng/mL), or their combination (0.3–30 ng/mL) for 24 hours Total RNA was isolated and real-time quantitative PCR for ICAM-1, VCAM-1, and GAPDH was performed. Data were analyzed by the comparative cycle threshold method and expressed as the fold index relative to the nonstimulated control (three trials). Values are means ± SD; $^*P < 0.05$, Student's t-test.

for 24 hours. Purified eosinophils from three different donors were preincubated with 1 ng/mL IL-5 for 15 minutes, then cocultured with the cultured fibroblasts (1×10^5 cells per well) for 3 hours The wells were washed gently with PBS to remove nonadhered eosinophils, and the eosinophils adhered to the fibroblasts were counted using the light microscope field. To determine the effect of two adhesion molecules, ICAM-1 and VCAM-1, on eosinophil-fibroblast interactions, an inhibition assay was performed using anti-ICAM-1 monoclonal antibody (mAb) and anti-VCAM-1 mAb. After stimulation of fibroblasts with IL-4 and TNF-α for 24 hours, 50 μL anti-mouse IgG_1 (Sigma), anti-ICAM-1 mAb, and anti-VCAM-1 mAb (Immunotech) were added and reacted for 30 minutes at 37°C before coculturing.

Morphologic Study of Fibroblasts Cocultured with Eosinophils

By a similar method as the adhesion assays, fibroblasts were cultured in 96-well plates and stimulated with IL-4 and/or TNF-α for 24 hours. Preactivated eosinophils were added to the cultured fibroblasts, and they were cocultured for 72 hours. After coculturing, fibroblasts were gently washed twice with PBS, then 20 μL of 0.5% trypan blue solution was added, and the cells were stained for 1 minute. After removing the solution with a pipet, nonstained cells, regarded as intact, were immediately counted under the microscope.

TUNEL Assay for Detection of Apoptosis in Fibroblasts

Apoptosis in the cocultures of fibroblasts with eosinophils was detected employing the TUNEL (terminal deoxynucleotidyl transferase [TdT]-mediated deoxyuridine triphosphate [dUTP] nick-end labeling) assay, using a commerically available kit (In Situ Cell Death Detection Kit, Peroxidase; Boehringer Mannheim, Mannheim, Germany) per manufacturer's instructions.

Repeatability of the Individual Experiments

Gene chip analysis, real-time PCR and flow cytometry experiments, adhesion assays, and morphologic studies were repeated three times in this study.

Conjunctival and Corneal Impression Cytology

Conjunctival and corneal impression cytology was performed on eight patients with AKC and corneal ulcers (8 eyes; 7 males, 1 female; mean age 24 years, range 9–34 years). The impression cytology specimens were obtained after administration of topical anesthesia with 0.4% oxybuprocaine. Strips of cellulose acetate filter paper (HAWP 304; Millipore, Bedford, MA) that were soaked in distilled water for a few hours and dried at room temperature were applied on upper palpebral conjunctiva and corneal ulcers, pressed gently by a glass rod, and then removed. The specimens were then fixed with formaldehyde. The specimens were stained with periodic acid schiff, dehydrated in ascending grades of ethanol and then with xylol, and finally coverslipped. The status of epithelial cells was determined by taking photographs using a light microscope at a magnification of 400×. The same researcher, who was masked to the identity of the specimen donors, evaluated the specimens for goblet cell counts, epithelial squamous metaplasia grades, and presence of inflammatory cell infiltrates.

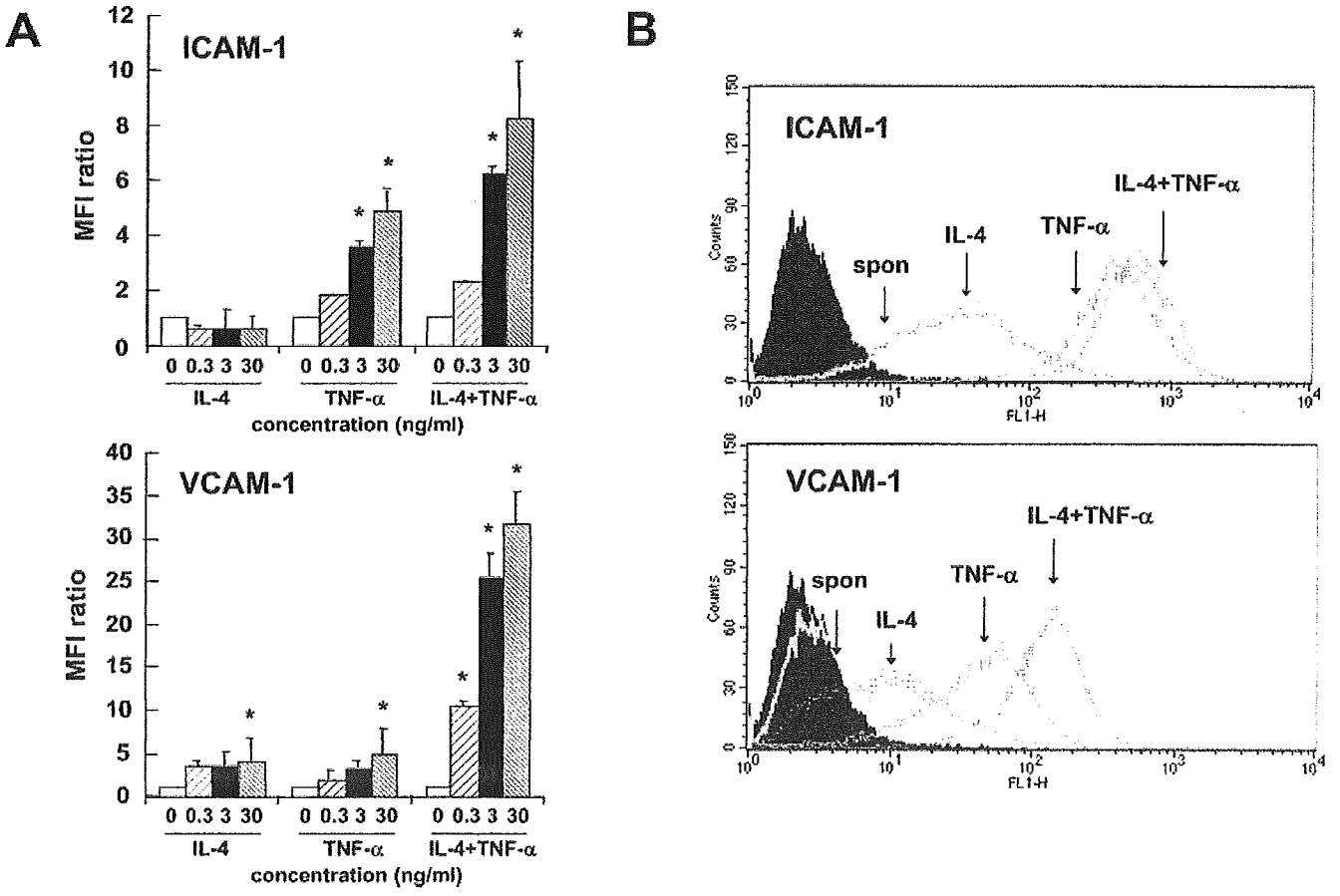

FIGURE 3. Flow cytometry analysis of the expression of ICAM-1 and VCAM-1 on corneal fibroblasts. Corneal fibroblasts were incubated with IL-4 (0.3–30 ng/mL), TNF-α (0.3–30 ng/mL), or their combination (0.3–30 ng/mL) at 37°C for 24 hours. Cells were washed and stained with anti-ICAM-1 mAb and anti-VCAM-1 mAb and analyzed by flow cytometry. IL-4 and TNF-α induced the expression of ICAM-1 and VCAM-1 on corneal fibroblasts. (**A**) Mean fluorescence intensity (MFI) of ICAM-1 and VCAM-1 in flow cytometry ($n = 3$); $^*P < 0.05$. (**B**) Representative individual fluorescence intensity profile of ICAM-1 and VCAM-1 in flow cytometry.

Statistical Analysis

All data are presented as means ± SEM. Depending on the distribution of the individual data, the significance of differences between groups was determined by either Student's *t*-test or a Mann–Whitney rank sum test. Repeated-measures ANOVA was used where more than one comparison was made. Values of $P < 0.05$ were considered significant.

Results

Real-Time PCR Analysis of ICAM-1 and VCAM-1 Expression after IL-4 and TNF-α Stimulation of Fibroblasts

A significant increase in both ICAM-1 and VCAM-1 mRNA expression over basal levels was observed with TNF-α (0.3–30 ng/mL) stimulation (4.8- and 4.6-fold, compared to control, at 30 ng/mL) as shown in Figure 2. Although IL-4 (0.3–30 ng/mL) alone did not enhance ICAM-1 mRNA expression, a combination of TNF-α and IL-4 showed a slight additive effect on ICAM-1 mRNA expression. In contrast, VCAM-1 mRNA expression was increased by IL-4 alone to the same extent as with TNF-α stimulation (4.0-fold, at 30 ng/mL). A combination of 30 ng/mL TNF-α and IL-4 resulted in the greatest augmentation of VCAM-1 mRNA expression (32-fold).

Flow Cytometry Analysis of ICAM-1 and VCAM-1 Expression on Corneal Fibroblasts

As shown in Figure 3, ICAM-1 was constitutively expressed on corneal fibroblasts, and significantly enhanced by TNF-α stimulation alone ($P < 0.05$) but not by IL-4 stimulation. Stimulation with the combination of IL-4 and TNF-α showed an additive effect on ICAM-1 expression. On the other hand, VCAM-1 was scarcely expressed on resting corneal fibroblasts, but was induced by IL-4 or TNF-α stimulation. A combination of IL-4 and TNF-α showed an additive effect on VCAM-1 expression.

Morphologic Analysis of Eosinophil Adhesion to Corneal Fibroblasts

When unstimulated fibroblasts were incubated with activated eosinophils (1×10^5 cells per well), slight spontaneous eosinophil adhesion to fibroblasts was noted at 20.3 ± 4.9 cells/high power field (hpf) (Fig. 4A). After preincubation of fibroblasts with IL-4 (1–100 ng/mL) or TNF-α (1–100 ng/mL) for 24 hours, the number of adhered eosinophils increased in a dose-dependent manner ($P < 0.001$). A combination of IL-4 and TNF-α showed an additive effect on eosinophil adhesion. After stimulation with both 100 ng/mL IL-4 and 100 ng/mL TNF-α, eosinophil adhesion was most enhanced at 99.0 ± 15.6 cells/hpf (a fivefold increase, compared with nonstimulated controls).

Morphologic Analysis of the Viability of Corneal Fibroblasts Cocultured with Eosinophils

In eosinophil adhesion assays, we observed slight morphologic changes in fibroblasts cocultured with eosinophils after 3 hours of incubation. Therefore, we continued the coculture study and observed the eosinophil-dependent morphologic changes in the fibroblasts. At 72 hours, corneal fibroblasts were partially damaged, and a number of cells were detached from the culture dish. After cocultured fibroblasts were gently washed with PBS, a trypan blue exclusion test was performed. The number of intact fibroblasts incubated without eosinophils was 44.0 ± 3.4 cells/hpf, and the viability was consistently 100%. It was also confirmed that IL-4 and TNF-α scarcely affected the viability of fibroblasts in our system (data not shown). Preincubation of fibroblasts with IL-4 or TNF-α increased the number of damaged cells in a concentration-dependent manner when cocultured with eosinophils (Fig. 4B). Preincubation with both 100 ng/mL IL-4 and 100 ng/mL TNF-α showed an additive effect on cell damage (53.7%).

All fibroblasts in IL-4– and TNF-α–stimulated cocultures with eosinophils were TUNEL negative and did not reveal specific features of apoptosis, such as shrinkage of cells or nuclear changes.

Morphologic Changes of Eosinophil Adhesion to Corneal Fibroblasts and Eosinophil-Induced Fibroblast Damage with Anti–ICAM-1 or Anti–VCAM-1 Treatment

The addition of anti–ICAM-1 mAb or anti–VCAM-1 mAb (10 μg/mL) significantly inhibited the adhesion of eosinophils to

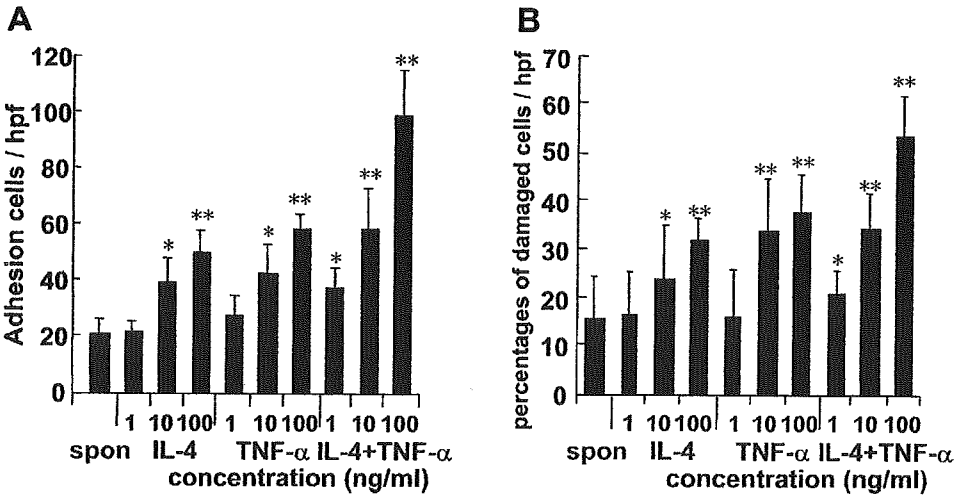

FIGURE 4. Morphologic analysis of eosinophil adhesion and fibroblast damage. Corneal fibroblasts were preincubated for 24 hours with IL-4 and/or TNF-α. Eosinophils primed with IL-5 were then added. (**A**) Graph shows the number of adhered eosinophils counted by light microscopic observation; eosinophil adhesion to corneal fibroblasts is significantly increased in stimulated cultures compared to control cultures ($n = 3$); $^*P < 0.05$, $^{**}P < 0.005$. (**B**) Eosinophils were incubated for 72 hours. Graph shows a significant increase of corneal fibroblast damage compared to control cultures. Percentages of damaged cells were calculated by subtraction of trypan blue–negative cells (100% = viability of control fibroblasts without addition of eosinophils and cytokines; $n = 3$); $^*P < 0.05$, $^{**}P < 0.005$. spon, spontaneous.

activated fibroblasts (Fig. 5A). Preincubation with anti-ICAM-1 or anti-VCAM-1 mAb significantly inhibited the eosinophil adhesion by approximately 80%, compared to the level observed with mouse IgG_1 application.

Eosinophil-induced cell damage was also assayed after 72 hours of coculturing. Treatment with anti-ICAM-1 mAb and anti-VCAM-1 mAb significantly reduced the fibroblast damage (57% and 43%, respectively) to a similar extent as with eosinophil adhesion (Fig. 5B). An additive reduction of fibroblast damage was observed when fibroblasts were treated with both anti-ICAM-1 and anti-VCAM-1 mAbs.

Conjunctival and Corneal Impression Cytology

To provide further evidence for our in vitro findings, conjunctival and corneal impression cytology was carried out on eight patients with AKC and sterile shield corneal ulceration (eight eyes). Conjunctival imprints from all eyes contained sheets of conjunctival epithelial cells with advanced squamous metaplasia, inflammatory cell infiltrates, predominant neutrophils and eosinophils, variable amounts of goblet cells, and mucin pickup. Figure 6A shows an abundance of inflammatory cell infiltrates, consisting mainly of neutrophils and eosinophils, adjacent to conjunctival epithelial cells with advanced squamous metaplasia (Dogru M, et al. *IOVS* 2002;46:ARVO E-Abstract 939). The red arrows indicate eosinophils, the black arrow points to a conjunctival epithelial sheet with Nelson's grade 2 squamous metaplasia and decreased cellular cohesion, and the black stars indicate a total loss of cellular cohesion between the focus of inflammation and the surrounding epithelial cells. The orange arrow indicates a loss of cellular cohesion between the conjunctival epithelial cells lying under the inflammatory infiltrates.

Imprints from eyes of patients with corneal ulcers revealed extensive infiltration by both neutrophils and eosinophils among isolated corneal epithelial cells with advanced squamous metaplasia. Figure 6B, a representative corneal impression cytology imprint obtained from the ulcer edge in the same patient as Figure 6A, shows extensive infiltration by eosinophils (red arrows) and neutrophils and isolated corneal epithelial cells with Nelson's grade 3 squamous metaplasia.

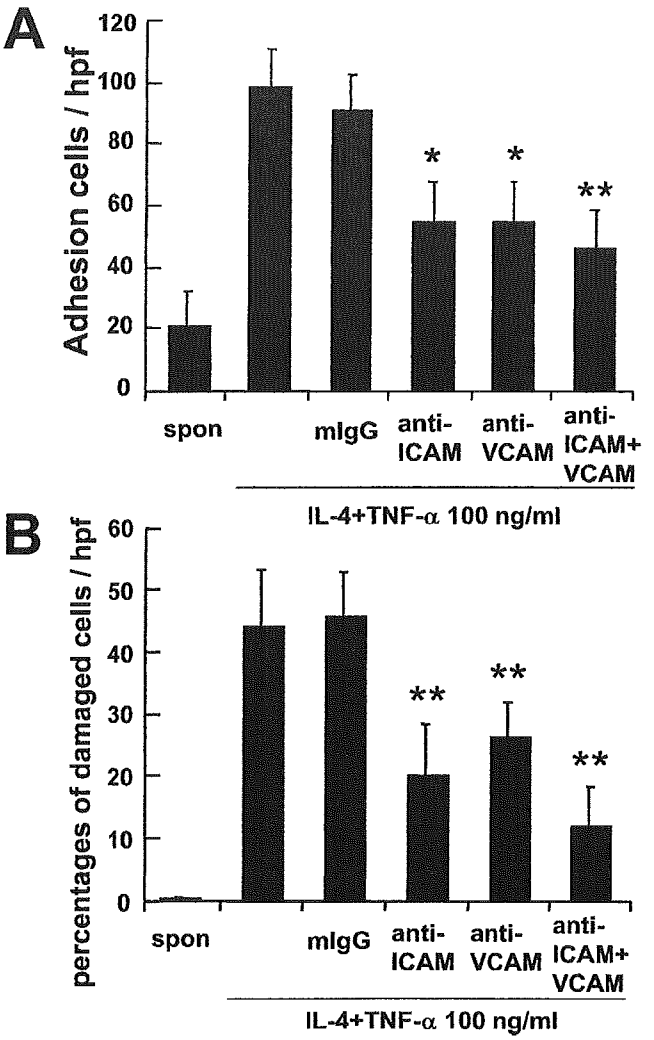

FIGURE 5. The effects of anti-ICAM-1 and anti-VCAM-1 mAb on cell adhesion and fibroblast damage. Cultured fibroblasts were treated with IL-4 and TNF-α (100 ng/mL each) and mouse IgG1 (mIgG; control), anti-ICAM-1, and anti-VCAM-1 antibody (10 mg/mL each) for 30 minutes. (**A**) Primed eosinophils were cocultured for 3 hours, and adhered eosinophils were counted ($n = 3$); $^*P < 0.05$, $^{**}P < 0.005$. (**B**) Primed eosinophils were cocultured for 72 hrs, and the viability of keratocytes was evaluated by counting trypan blue-negative cells. Percentage of damaged cells was calculated by subtraction of trypan blue-negative cells ($n = 3$); $^{**}P < 0.005$. spon, spontaneous.

DISCUSSION

Eosinophils have long been blamed for the morbidity of corneal complications in patients with allergies. Indeed, eosinophils have been shown to accumulate on the ocular surface in patients with allergic conjunctivitis and to exert cytotoxic effects through degranulation. We have previously reported higher concentrations of eotaxins in the tears of patients with severe ocular allergies and observed that tears of such patients had chemotactic activity for eosinophils in vitro.[6] Although the current literature suggests some evidence in relation to eosinophil-induced ocular damage in ocular surface allergies, the precise mechanisms of the formation of severe corneal damage, especially corneal ulceration, are still not clear.

Therefore, we performed quantitative real-time PCR and flow cytometric analysis to confirm the expression of ICAM-1 and VCAM-1 related to eosinophils at the mRNA and protein levels. We also looked into the in vitro morphologic alterations of corneal fibroblasts cocultured with eosinophils by assessing eosinophil adhesion to corneal fibroblasts, fibroblast viability, and the effects of anti-ICAM-1 and anti-VCAM-1 treatment on fibroblast morphology.

It is well known that keratocyte apoptosis is one the first events to follow corneal epithelial injury. Virtually any source of corneal epithelial injury, such as a mechanical scrape, LASIK surgery, or an infectious process, causes the release of cytokines from the epithelium, resulting in the activation and transformation of keratocytes into a repair phenotype of fibroblasts that release enzymes such as collagenases, matrix metalloproteinases involved in stromal modeling.[33] We thus chose to use fibroblast instead of keratocyte cultures in this study to investigate active fibroblast-related events that may be important in allergic wound-healing response. To support the findings from the in vitro experiments of this study, we performed conjunctival and corneal impression cytology on AKC patients with corneal ulcers as well.

We initially confirmed the expression of two adhesion molecules, ICAM-1 and VCAM-1, by real-time PCR and flow cytometry. Real-time PCR provided evidence that ICAM-1 and VCAM-1 mRNA expression were upregulated with IL-4 and TNF-α stimulation. Flow cytometry analysis revealed further evidence of increased corneal fibroblast expression of ICAM-1 and VCAM-1 on stimulation by IL-4 and TNF-α. We thought that increased expression of ICAM-1 and VCAM-1 on corneal fibroblasts on stimulation with IL-4 and TNF-α, two cytokines

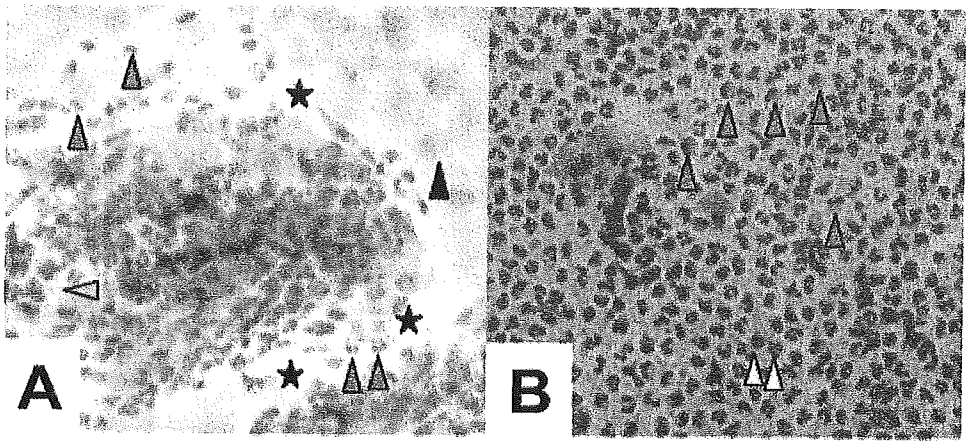

FIGURE 6. (A) Conjunctival impression cytology specimen from a patient with AKC and corneal ulceration, showing the abundance of inflammatory cell infiltrates, consisting mainly of neutrophils and eosinophils (*red arrows*), adjacent to conjunctival epithelial cells with advanced Nelson's grade 2 squamous metaplasia and decreased cellular cohesion (*black arrow*), as well as the total loss of cellular cohesion between the focus of inflammation and the surrounding epithelial cells (*black stars*) and the loss of cellular cohesion between the conjunctival epithelial cells lying under the inflammatory infiltrates (*orange arrow*) (magnification, ×100). (B) Representative corneal impression cytology imprint obtained from the ulcer edge in the same patient, showing extensive eosinophilic infiltration (*red arrows*) and neutrophils (*yellow arrows*) and isolated corneal epithelial cells with Nelson's grade 3 squamous metaplasia (Wiegert's iron hematoxylin staining; magnification, ×100) (Dogru M, et al. *IOVS* 2002;46:ARVO E-Abstract 939).

known to be present in high amounts in allergic ocular surfaces, prepared a background which would ease the adhesion of eosinophils to corneal fibroblasts.

Indeed, eosinophils are known to bind ICAM-1 via all four members of the CD18 integrin family, CD11a to -d, which are expressed on the eosinophil cell sulface.[22–27] Eosinophils also express a number of $\beta 1$ integrins, of which $\alpha 4\beta 1$, the ligand of VCAM-1, is best characterized.[28] Observations from previous studies suggest that ICAM-1 and VCAM-1 are the potent molecules involved in eosinophil-fibroblast adhesion. The present study is the first to describe the morphologic alterations of corneal fibroblasts exposed to IL-4 and TNF-α, and bound by eosinophils.

Our morphologic observations of the cocultures showed that both IL-4 and TNF-α increased eosinophil adhesion to corneal fibroblasts solitarily and in combination. Likewise, applications of both cytokines were associated with significant increases in corneal fibroblast cell damage in the cultures. Our TUNEL assay findings suggested that fibroblast cellular damage was due to eosinophil-induced necrosis rather than apoptosis. Interestingly, blocking experiments performed with anti-ICAM-1 and anti-VCAM-1 applications revealed partial reversal of cellular damage. The reversal effect was enhanced when anti-ICAM-1 and anti-VCAM-1 were applied concomitantly.

Our results suggest that eosinophil adhesion to corneal fibroblasts via ICAM-1 and VCAM-1 may lead to degranulation of eosinophils. Indeed, eosinophils contain cytotoxic proteins such as ECP and MBP, which are released on activation and have been reported to cause damage to corneal cellular structures.[12] However, it should be noted that eosinophil adhesion was not completely inhibited with the anti-ICAM-1 and anti-VCAM-1 monoclonal antibodies in this study, indicating that other molecules may be associated with corneal fibroblasts. Recent evidence indicates that cell adhesion through CD11b/CD18 (Mac-1) is a crucial step for the activation, signaling, and effector function of eosinophils.[20,21] On the other hand, it has been reported that VLA-4 (CD49d)-mediated adhesion augments stimulated eosinophil degranulation. Therefore, ICAM-1/$\beta 2$ and VCAM-1/VLA-4 interactions seem to be involved in the mechanisms of eosinophil cytotoxicity.

Conjunctival impression cytology findings in all subjects revealed inflammatory cell infiltrates, consisting mainly of neutrophils and eosinophils, adjacent to conjunctival epithelial cells with advanced squamous metaplasia, providing clinical evidence on the adverse effects of the inflammatory process on the epithelial cells and backing up our findings from the in vitro experiments. Interestingly, imprints obtained from corneal ulcers showed extensive eosinophilic and neutrophilic infiltration among isolated corneal epithelial cells with advanced squamous metaplasia, suggesting adverse effects of the infiltrates on cellular cohesion and integrity.

In conclusion, we found that corneal fibroblasts express ICAM-1 and VCAM-1 when activated with IL-4 and TNF-α, and the expression is highly selective among all adhesion-related molecules. Eosinophils can adhere to the activated fibroblasts and can induce subsequent fibroblast damage through the adhesion molecules. Eosinophil adhesion to fibroblasts may contribute to the pathogenesis of severe persistent allergic corneal ulcers.

References

1. Matsumoto K, Saito H. The role of eosinophils in asthma: Sarastro or the Queen of the Night? *Int Arch Allergy Immunol.* 2001;125:290–296.
2. Foster CS, Calonge M. Atopic keratoconjunctivitis. *Ophthalmology.* 1990;97:992–1000.
3. Tuft SJ, Kemeny DM, Dart JK, Buckley RJ. Clinical features of atopic keratoconjunctivitis. *Ophthalmology.* 1991;98:150–158.
4. Cameron JA. Shield ulcers and plaques of the cornea in vernal keratoconjunctivitis. *Ophthalmology.* 1995;102:985–993.
5. Montan PG, Biberfeld PJ, Scheynius A. IgE, IgE receptors, and other immunocytochemical markers in atopic and nonatopic patients with vernal keratoconjunctivitis. *Ophthalmology.* 1995;102:725–732.
6. Fukagawa K, Nakajima T, Tsubota K, Shimmura S, Saito H, Hirai K. Presence of eotaxin in tears of patients with atopic keratoconjunctivitis with severe corneal damage. *J Allergy Clin Immunol.* 1999;103:1220–1221.
7. Eidelman DH, Minshall E, Dandurand RJ, et al. Evidence for major basic protein immunoreactivity and interleukin 5 gene activation during the late phase response in explanted airways. *Am J Respir Cell Mol Biol.* 1996;15:582–589.
8. Tsubota K, Takamura E, Hasegawa T, Kobayashi T. Detection by brush cytology of mast cells and eosinophils in allergic and vernal conjunctivitis. *Cornea.* 1991;10:525–531.
9. Montan PG, van Hage-Hamsten M. Eosinophil cationic protein in tears in allergic conjunctivitis. *Br J Ophthalmol.* 1996;80:556–560.
10. Leonardi A, Borghesan F, Faggian D, Secchi A, Plebani M. Eosinophil cationic protein in tears of normal subjects and patients affected by vernal keratoconjunctivitis. *Allergy.* 1995;50:610–613.
11. Trocme SD, Kephart GM, Bourne WM, Buckley RJ, Gleich GJ. Eosinophil granule major basic protein deposition in corneal ulcers associated with vernal keratoconjunctivitis. *Am J Ophthalmol.* 1993;115:640–643.
12. Trocme SD, Hallberg CK, Gill KS, Gleich GJ, Tyring SK, Brysk MM. Effects of eosinophil granule proteins on human corneal epithelial cell viability and morphology. *Invest Ophthalmol Vis Sci.* 1997;38:593–599.

13. Fujishima H, Takeuchi T, Shinozaki N, Saito I, Tsubota K. Measurement of IL-4 in tears of patients with seasonal allergic conjunctivitis and vernal keratoconjunctivitis. *Clin Exp Immunol.* 1995; 102:395–398.
14. Leonardi A, Borghesan F, DePaoli M, Plebani M, Secchi AG. Procollagens and inflammatory cytokine concentrations in tarsal and limbal vernal keratoconjunctivitis. *Exp Eye Res.* 1998;67:105–112.
15. Fukagawa K, Nakajima T, Saito H, et al. IL-4 induces eotaxin production in corneal keratocytes but not in epithelial cells. *Int Arch Allergy Immunol.* 2000;121:144–150.
16. Piela-Smith TH, Broketa G, Hand A, Korn JH. Regulation of ICAM-1 expression and function in human dermal fibroblasts by IL-4. *J Immunol.* 1992;148:1375–1381.
17. Fukagawa K, Okada N, Fujishima H, et al. CC-chemokine receptor 3: a possible target in treatment of allergy-related corneal ulcer. *Invest Ophthalmol Vis Sci.* 2002;43:58–62.
18. Xu X, Hakansson L. Regulation of the release of eosinophil cationic protein by eosinophil adhesion. *Clin Exp Allergy.* 2000;30:794–806.
19. Munoz NM, Hamann KJ, Rabe KF, Sano H, Zhu X, Leff AR. Augmentation of eosinophil degranulation and LTC(4) secretion by integrin-mediated endothelial cell adhesion. *Am J Physiol.* 1999; 277:L802–L810.
20. Horie S, Kita H. CD11b/CD18 (Mac-1) is required for degranulation of human eosinophils induced by human recombinant granulocyte-macrophage colony-stimulating factor and platelet-activating factor. *J Immunol.* 1994;152:5457–5467.
21. Kaneko M, Horie S, Kato M, Gleich GJ, Kita H. A crucial role for beta 2 integrin in the activation of eosinophils stimulated by IgG. *J Immunol.* 1995;155:2631–2641.
22. Hartnell A, Moqbel R, Walsh GM, Bradley B, Kay AB. Fc gamma and CD11/CD18 receptor expression on normal density and low density human eosinophils. *Immunology.* 1990;69:264–270.
23. Walsh GM, Wardlaw AJ, Hartnell A, Sanderson CJ, Kay AB. Interleukin-5 enhances the in vitro adhesion of human eosinophils, but not neutrophils, in a leucocyte integrin (CD11/18)-dependent manner. *Int Arch Allergy Appl Immunol.* 1991;94:174–178.
24. Lo SK, Detmers PA, Levin SM, Wright SD. Transient adhesion of neutrophils to endothelium. *J Exp Med.* 1989;169:1779–1793.
25. Diamond MS, Springer TA. A subpopulation of Mac-1 (CD11b/CD18) molecules mediates neutrophil adhesion to ICAM-1 and fibrinogen. *J Cell Biol.* 1993;120:545–556.
26. Staunton DE, Dustin ML, Springer TA. Functional cloning of ICAM-2, a cell adhesion ligand for LFA-1 homologous to ICAM-1. *Nature.* 1989;339:61–64.
27. de Fougerolles AR, Springer TA. Intercellular adhesion molecule 3, a third adhesion counter-receptor for lymphocyte function-associated molecule 1 on resting lymphocytes. *J Exp Med.* 1992;175:185–190.
28. Nagata M, Sedgwick JB, Bates ME, Kita H, Busse WW. Eosinophil adhesion to vascular cell adhesion molecule-1 activates superoxide anion generation. *J Immunol.* 1995;155:2194–2202.
29. Takafuji S, Shoji S, Ito K, Yamamoto K, Nakagawa T. Eosinophil degranulation in the presence of lung fibroblasts. *Int Arch Allergy Immunol.* 1998;117(suppl 1):52–54.
30. Hansel TT, De Vries IJ, Iff T, et al. An improved immunomagnetic procedure for the isolation of highly purified human blood eosinophils. *J Immunol Methods.* 1991;145:105–110.
31. Di Nardo A, Vitiello A, Gallo RL. Cutting edge: mast cell antimicrobial activity is mediated by expression of cathelicidin antimicrobial peptide. *J Immunol.* 2003;170:2274–2278.
32. Razzaque MS, Foster CS, Ahmed AR. Role of collagen-binding heat shock protein 47 and transforming growth factor-beta1 in conjunctival scarring in ocular cicatricial pemphigoid. *Invest Ophthalmol Vis Sci.* 2003;44:1616–1621.
33. Wilson SE, Mohan RR, Hong JW, Lee JS, Choi R, Mohan RR. The wound healing response after lasik in situ keratomilieusis and photorefractive keratectomy. *Arch Ophthalmol.* 2001;119:889–896.

SCIENTIFIC REPORT

Transplantation of corneal endothelium with Descemet's membrane using a hyroxyethyl methacrylate polymer as a carrier

S Shimmura, H Miyashita, K Konomi, N Shinozaki, T Taguchi, H Kobayashi, J Shimazaki, J Tanaka, K Tsubota

Br J Ophthalmol 2005;**89**:134–137. doi: 10.1136/bjo.2004.050591

Aims: To evaluate the histology and function of Descemet's membrane transplanted with intact endothelium.

Methods: Japanese white rabbits and human eyebank eyes were used as donors and recipients of Descemet's membrane transplantation. Donor endothelium was hydrodissected by injecting indocyanine green from a limbal incision, and then processed as a corneal scleral button. A 6 mm diameter donor sheet was trephined, and folded in half using a 6 mm diameter polymer as a carrier. Recipient endothelium was also hydrodissected from the limbus using trypan blue to stain the Descemet's membrane. Continuous curvilinear descemetorhexis (CCD) was performed to remove a circular section of the Descemet's membrane using a 27 gauge cystotome. Donor tissue was inserted into the anterior chamber through a 5 mm limbal incision and apposed to the host stroma. Polymers were removed following transplantation. Similar surgical procedures were performed in both rabbits and eyebank eyes. Haematoxylin eosin stains were performed after 28 days in rabbits, and eyebank eyes were fixed immediately following surgery for endothelial cell counts.

Results: Rabbit control eyes demonstrated stromal oedema caused by loss of Descemet's membrane, whereas transplanted eyes had clear corneas. The mean (standard deviation) pachymetry of operated eyes was 376.6 (SD 32.5) μm compared with 389.6 (SD 25.1) μm in the unoperated eye. Mean endothelial density immediately following surgery in eyebank eyes was 2749 (SD 288) cells/mm^2.

Conclusions: Transplantation of Descemet's membrane by CCD produces a functional graft with an optically clear interface similar to control cornea.

Penetrating keratoplasty (PKP) has a long history as a surgical technique to treat irreversible opacification of the cornea. PKP is still the first choice of surgery for a wide range of diseases including bullous keratopathy, dystrophies, keratoconus, and trauma. However, damage spanning the entire thickness of the cornea from epithelium to endothelium is a relatively rare occurrence. For diseases other than bullous keratopathy, techniques such as deep lamellar keratoplasty (DLKP)[1 2] or epithelial sheet transplantation[3 4] are new alternatives to PKP in which only damaged tissue is surgically replaced. Similarly, the stroma and epithelium are not necessary in the treatment of bullous keratopathy, where only the endothelium is compromised by disease or injury. Several studies have shown the feasibility of transplanting posterior lamellar tissue instead of PKP.

One such technique is endothelial lamellar keratoplasty which uses a microkeratome to create a flap, followed by the replacement of posterior lamellar tissue taken from a donor cornea.[5 6] The use of a microkeratome leaves little opacification of the stromal interface, and a large flap covering the donor offers greater adhesive strength than running sutures used in PKP. Another method for transplanting endothelial tissue with a thin layer of stroma used as a carrier was reported by Melles *et al*.[7] The technique was further refined to allow transplantation through a small limbal incision—as opposed to a large wound reported in the original technique.[8] Initial clinical results are promising; however, manual lamellar incision of the stroma may cause mild haze in the stromal interface.

The adhesion between Descemet's membrane (DM) and posterior stroma is not anatomically strong, so the membrane can be peeled off without much effort. This is done when removing donor endothelium from a DLKP donor button before transplantation.[9] DM can also be detached by hydrodissection or viscodissection to obtain a smooth interface at the plane separating DM and stroma.[10] Our experience with DLKP by hydrodissection led to a new technique to obtain controlled sizes of DM by hydrodissecion followed by continuous curvilinear descemetorhexis (CCD). However, Descemet's membrane alone has the tendency to curl into a tube-like structure with the endothelial cells facing outwards. In order to control the plasticity of DM, we used polymers as a carrier during insertion and spreading of DM. In the present study, we show the histopathological and functional results of endothelial transplantation in rabbit and human eye bank eyes by this technique.

METHODS

Japanese white rabbits (female, 3 kg body weight, Shiraishi experimental animal breeding farm, Tokyo, Japan) were used as an animal model for endothelial transplantation. All animals were treated according to the ARVO Statement for the Use of Animals in Ophthalmology and Vision Research. Recipient animals (n = 4) were anaesthetised with 4 ml intramuscular ketamine and xylazine (1:7 mixture) and topical xylocain. To limit the extensive fibrin response observed in rabbits, pupils were expanded with topical tropicamide, and the anterior chamber was irrigated with heparin (5 U/ml). A 5 mm incision was made at the corneoscleral rim down to the plane of Schlemm's canal, and DM was hydrodissected by injecting 0.04% trypan blue into the supra Descemet space using a blunt 27 gauge needle (fig 1A–C). Following injection of air into the anterior

Abbreviations: CCD, continuous curvilinear descemetorhexis; DLKP, deep lamellar keratoplasty; DM, Descemet's membrane; HE, haematoxylin eosin; PKP, penetrating keratoplasty.

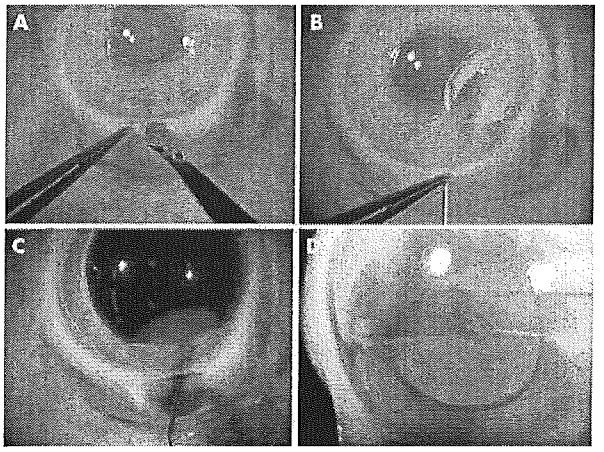

Figure 1 Surgical procedure for preparing the recipient shown in a rabbit eye. (A) An incision was made down to the plane of DM. (B), (C) Hydrodissection of DM is performed with balanced salt solution followed by trypan blue. (D) After removing trypan blue dye, a cystotome is inserted into the anterior chamber to perform CCD. The same procedure was performed in eyebank eyes.

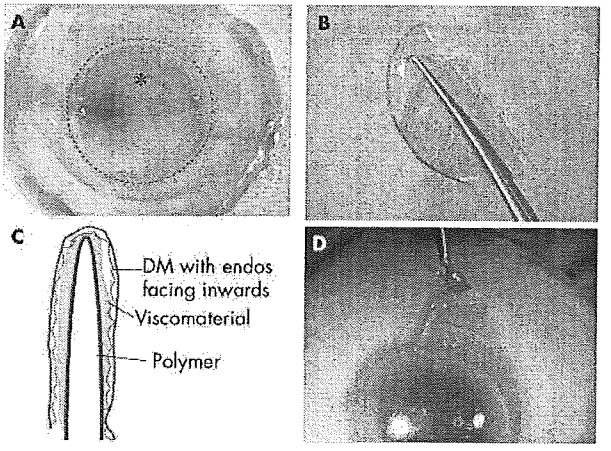

Figure 2 Preparation of donor tissue shown in an eyebank eye. (A) Donor DM is dissected with indocyanine green as described in figure 1, processed into a corneoscleral button, and trephined so that an incision is made in DM (dotted circle). Viscomaterial is coated on the endothelial surface and a hyroxyethyl methacrylate polymer carrier (*) is folded in half and placed on DM. (B) Capsulorrhexis forceps used to grasp the polymer/DM composite with endothelial cells facing inwards. (C) A cross sectional schematic view of polymer/DM shown in (B). (D) The polymer is removed after DM is placed in position with the use of air. The same procedure was performed in rabbits.

chamber, CCD was performed to remove a circular section of the Descemet's membrane using a 27 gauge cystotome (fig 1D).

Two animals were sacrificed using an overdose of pentobarbital at the time of surgery to provide a total of four donor buttons. Following enucleation of the donor globe, a 3 mm incision was made at the corneoscleral rim, and DM was hydrodissected by injecting 6.25 mg/ml indocyanine green so that the donor and recipient DM could be differentiated by colour. After creating a corneal scleral button, a 6 mm diameter incision was made in the DM using a manual trephine, and the endothelium was coated with viscoelastic material to protect the cells from physical friction. The polymer/DM composite was folded in half using an 8 mm diameter hyroxyethyl methacrylate polymer (one day ACUVUE; Johnson and Johnson, Jacksonville, FL, USA) as a carrier (fig 2A). The polymer/DM with endothelial cells facing inward was grasped with capsulorrhexis forceps towards the leading edge of the polymer (fig 2B, C). Donor tissue with the polymer carrier was inserted into the anterior chamber filled with air through the 5 mm limbal incision, and apposed to the host stroma by expanding the polymer. Additional air is injected into the anterior chamber to further adhere the DM to the posterior stromal surface. Polymers were removed at the end of surgery. Control animals (n = 4) were operated by CCD alone without transplantation of donor endothelium, and another four rabbits served as sham negative control. All animals received topical antibiotics (levofloxacin) and steroids (betamethasone). After observing the rabbits for 28 days, animals were sacrificed and recipient corneas were fixed with 10% formalin over night. Paraffin sections were stained with haematoxylin and eosin.

Human eye bank eyes (five donors globes, five recipient globes) were obtained from the Northwest Lions Eyebank (Seattle, WA, USA). Donor DM were transplanted into five globes according to the procedure described above. Transplanted eyes were immediately processed into corneal scleral buttons for histological analysis of the transplanted endothelium. Following fixation with 4% paraformaldehyde, endothelial cell density was calculated by staining the nuclei of cells with 4', 6-diamidino-2-phenylindole dihydrochloride (DAPI, Dojindo Laboratories, Kumamoto, Japan) and analysed using the NIH Image software (National Institute of Health, Bethesda, MA, USA).

RESULTS

Endothelial transplantation in rabbits

The left eyes of four rabbits were transplanted with donor DM. Figure 3A shows a transplanted eye following surgery; the transplanted DM is stained green and the host DM is stained blue. Figure 3B shows the transplanted eye with a clear central cornea 28 days following surgery. Control eyes (fig 3C) had extensive stromal oedema with minimal view of the anterior chamber. The mean (standard deviation) pachymetry reading of transplanted eyes was 407.2 (SD 63.0) μm, which was not significantly different compared with sham operated controls with an average thickness of 391.2 (SD 20.8) μm. Positive control eyes operated by CCD alone were too oedematous to obtain readings with the pachymeter used in our study. The mean cell density in the rabbit eye 28 days after surgery was 2201.3 (SD 441.5) cells/

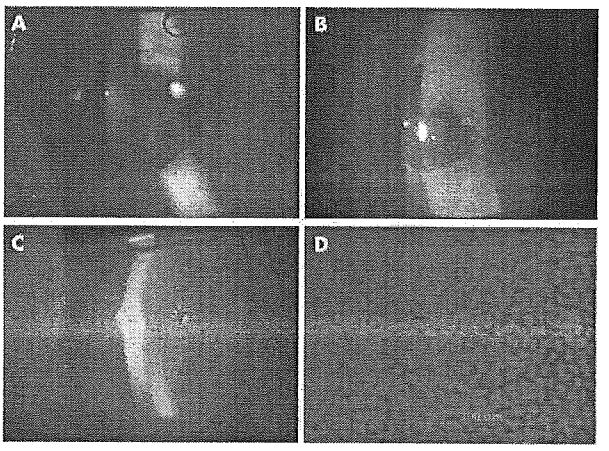

Figure 3 Postoperative eye in a rabbit with DM transplantation immediately following surgery (A) and after 28 days (B). Control eyes stripped of DM had extensive stromal oedema and opacification (C). Histology of endothelium within the graft shows a uniform layer of endothelium (D).

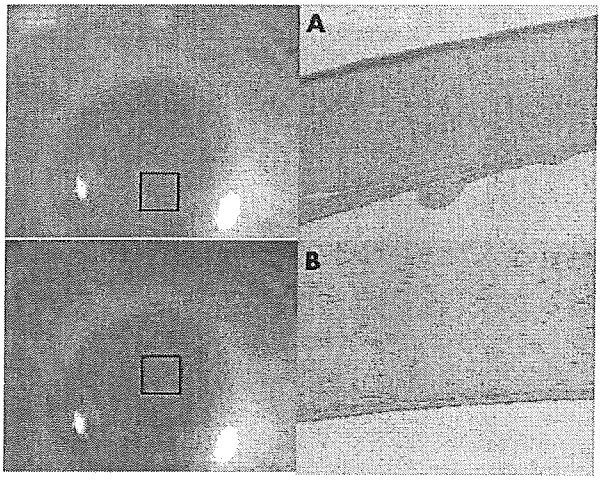

Figure 4 HE stains of the edge (A) and centre (B) of donor show a well apposed DM with slight curling of the edge. Original magnification (×100) for HE stains.

mm^2 (fig 3D) compared with 3180.5 (SD 98.2) cells/mm^2 in sham control. Cell loss was greater in rabbit eyes compared with eye bank eyes because of the very shallow anterior chambers in rabbits, which was an obstacle during surgical procedures.

Animals were sacrificed after 28 days, and the transplanted eyes were processed for histological examination. Haematoxylin eosin (HE) stains of the peripheral graft show a slightly curled edge of the transplanted DM (fig. 4A). The central graft is attached to the host stroma (fig 4B), which under high magnifications shows how the transplanted DM resembles DM in sham operated controls (fig 5). There was no observable infiltration of inflammatory cells in any of the operated eyes after 28 days.

Endothelial transplantation in human eyebank eyes

A total of five "donors" were transplanted into another five eyebank eyes using the same procedure explained in detail above. Corneal scleral rims were processed immediately following implantation to show the positioning of the graft (fig 6). Nuclear stains using DAPI revealed an endothelial cell density of 2749 (SD 288) cells/mm^2, suggesting that an adequate density of endothelial cells can be transplanted using this technique. No information was available as to the cell density of the eyes before the experiment; therefore the endothelial cell loss rate was not calculated.

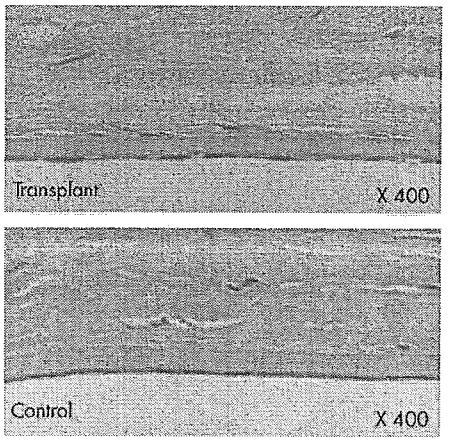

Figure 5 Higher magnification (×400) of the central graft reveals similar histological findings in both the transplanted eye and control.

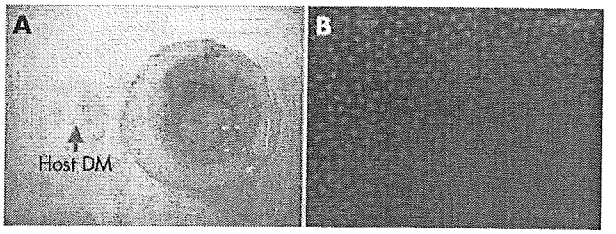

Figure 6 DM transplantation in human eyebank eye with green donor DM and blue recipient DM following CCD (A). Average endothelial density immediately following insertion of donor DM was 2749 (SD 288) cells/mm^2.

DISCUSSION

Surgical techniques in keratoplasty have changed over the past few years towards reducing tissue damage to a minimum, while transplanting only the layers of the cornea that are necessary for the particular patient. For stromal diseases such as keratoconus and the various dystrophies, DLKP can remove all of the stroma while leaving the host endothelium intact.[1,2] Epithelial transplants using amniotic membrane carriers are already in clinical use for the treatment of acute phase burns and Stevens Johnson syndrome with persistent epithelial defects.[11] The same technique can also be used to restore vision in the chronic stage of cicatricial disease such as ocular cicatricial pemphigoid, if the indications are chosen carefully.

Bullous keratopathy, however, is still mainly treated by PKP as the techniques involved in transplanting endothelium were believed to be technically difficult. Several experimental reports using animals have attempted to transplant endothelium by seeding the cells on hydrogel polymers,[12] or by using bovine DM as carriers.[13] More recently, clinical studies have described techniques to transplant the posterior stroma, including the endothelium, into bullous keratopathy patients. One technique is reported by Azar *et al*, who used a microkeratome to create a flap so that the posterior half of the donor cornea could be transplanted beneath the flap.[6] Our experience with the technique is favourable, with a clear optical interface between the host and donor. However, epithelial ingrowth can be a complication, and the need of a keratome can be costly. Another method described by Melles *et al* uses a spatula to dissect the host Descemet's membrane, after which a donor DM is inserted into the anterior chamber though a small corneal scleral incision.[7,8] The procedure seems promising in terms of refraction; however, stromal haze in the donor-host interface may occur when a spatula or knife is used to create a lamellar incision in the deep stroma. A custom made scraper was recently reported by the same group, which may solve these issues in the repicient stromal bed.[14]

The method described in this study uses hydrodissection to dissociate Descemet's membrane in both the donor and host, without the use of special instruments. This creates clear cut dissociation at the interface of DM and stroma, because fluid enters into the plane of weakest adhesion. The interface in this case is smoother than other methods using blades or spatula and, furthermore, does not interrupt the posterior stroma that contains keratocytes which may become activated to cause tissue reaction. The high magnification in figure 5 shows how the transplanted DM is closely apposed to the host stroma with little cellular infiltration or scarring in the posterior stroma. The grafts in rabbits show no interface

opacity under slit lamp examination, and the endothelial cell count is within an acceptable range. The average cell density in rabbits was lower than human eyebank eyes in our study, which was due to the fact that surgical manipulation was much more difficult in rabbits, which have very shallow anterior chambers and show fibrinotic response during surgery.

The rabbit data show that transplanted DM is functional, and that little tissue reaction is observed at the host-donor junction. However, as rabbit endothelial cells are known to proliferate in vivo, the same experiment was done using human eyebank eyes. The objective was to simulate a clinical situation, and also to assess the loss of endothelial cells during the procedure. As shown in figure 6, controlling the size and apposition of donor DM is possible, and the average endothelial cell density was above 2500 cells/mm^2. The preoperative endothelial density was not available; however, considering that the eyes were preserved in moist chambers without the use of storage medium, the results can be said to be more than adequate.

The largest obstacle to manipulating DM is the tendency for the 10 µm thick membrane to curl up with the endothelium facing outwards. Melles *et al* have developed an injector for the purpose of inserting the membrane into the anterior chamber.[10] We have shown that a hydroxyethyl methacrylate polymer can be used as a carrier by folding the DM in half, and also protect the graft from the loss of endothelial cells during insertion into the anterior chamber. The polymer can then be unfolded in the anterior chamber, and also be used to appose the DM to the stroma. The inserted DM is unfolded using a spatula inserted into the plane opposite the endothelium. Although the donor edge is not necessarily a perfect fit with the recipient bed (fig 4), the adhesion of donor DM is firm as evidenced from the fact that the membrane remains attached following paraffin fixation during HE stains. The report by Melles *et al* also shows that a perfect match is not necessary.

Transplantation of hydrodissected DM is an effective means to reproduce the normal anatomy of the posterior stroma. The hydrostatic pressure exerted by the endothelial pump is sufficient for the immediate attachment of the donor DM, and a polymer carrier offers protection and a means to insert DM through a small surgical wound. Encouraged by the results of this study, we are currently preparing a clinical trial based on the surgical technique described here.

Authors' affiliations
S Shimmura, H Miyashita, K Konomi, N Shinozaki, J Shimazaki, K Tsubota, Department of Ophthalmology, Tokyo Dental College, Chiba, Japan
T Taguchi, H Kobayashi, J Tanaka, Biomaterials Center, National Institute for Materials Science, Ibaragi, Japan
K Tsubota, Department of Ophthalmology, Keio University, Tokyo, Japan

This study was supported by The Advanced and Innovational Research Program in Life Sciences from the Japanese Ministry of Education, Culture, Sports, Science and Technology.

Correspondence to: Dr S Shimmura, Department of Opthalmology, Toyko Dental College, 5-11-13 Sugano, Ichikiawa, Chiba 272-8513, Japan; shimmura@tdc.ac.jp

Accepted for publication 7 July 2004

REFERENCES

1 **Aggarwal RK.** Deep lamellar keratoplasty—an alternative to penetrating keratoplasty. *Br J Ophthalmol* 1997;**81**:178–9.
2 **Sugita J,** Kondo J. Deep lamellar keratoplasty with complete removal of pathological stroma for vision improvement. *Br J Ophthalmol* 1997;**81**:184–8.
3 **Tsai RJ,** Li LM, Chen JK. Reconstruction of damaged corneas by transplantation of autologous limbal epithelial cells. *N Engl J Med* 2000;**343**:86–93.
4 **Rama P,** Bonini S, Lambiase A, *et al.* Autologous fibrin-cultured limbal stem cells permanently restore the corneal surface of patients with total limbal stem cell deficiency. *Transplantation* 2001;**72**:1478–85.
5 **Busin M,** Arffa RC, Sebastiani A. Endokeratoplasty as an alternative to penetrating keratoplasty for the surgical treatment of diseased endothelium: initial results. *Ophthalmology* 2000;**107**:2077–82.
6 **Azar DT,** Jain S, Sambursky R, *et al.* Microkeratome-assisted posterior keratoplasty. *J Cataract Refract Surg* 2001;**27**:353–6.
7 **Melles GR.** Posterior lamellar keratoplasty. *Arch Soc Esp Oftalmol* 2002;**77**:175–6.
8 **Melles GR,** Lander F, Nieuwendaal C. Sutureless, posterior lamellar keratoplasty: a case report of a modified technique. *Cornea* 2002;**21**:325–7.
9 **Shimmura S,** Shimazaki J, Tsubota K. Therapeutic deep lamellar keratoplasty for cornea perforation. *Am J Ophthalmol* 2003;**135**:896–7.
10 **Melles GR,** Lander F, Rietveld FJ. Transplantation of Descemet's membrane carrying viable endothelium through a small scleral incision. *Cornea* 2002;**21**:415–18.
11 **Koizumi N,** Inatomi T, Suzuki T, *et al.* Cultivated corneal epithelial transplantation for ocular surface reconstruction in acute phase of Stevens-Johnson syndrome. *Arch Ophthalmol* 2001;**119**:298–300.
12 **Mohay J,** Lange TM, Soltau JB, *et al.* Transplantation of corneal endothelial cells using a cell carrier device. *Cornea* 1994;**13**:173–82.
13 **Lange TM,** Wood TO, McLaughlin BJ. Corneal endothelial cell transplantation using Descemet's membrane as a carrier. *J Cataract Refract Surg* 1993;**19**:232–5.
14 **Melles GR,** Wijdh RH, Nieuwendaal CP. A technique to excise the descemet membrane from a recipient cornea (descemetorhexis). *Cornea* 2004;**23**:286–8.

Critical Role of the Fifth Domain of E-Cadherin for Heterophilic Adhesion with $\alpha_E\beta_7$, But Not for Homophilic Adhesion

Kiyono Shiraishi,[1]*† Kensei Tsuzaka,*† Keiko Yoshimoto,† Chika Kumazawa,*† Kyoko Nozaki,*† Tohru Abe,† Kazuo Tsubota,‡ and Tsutomu Takeuchi*†

The integrin $\alpha_E\beta_7$ is expressed on intestinal intraepithelial T lymphocytes and $CD8^+$ T lymphocytes in inflammatory lesions near epithelial cells. Adhesion between $\alpha_E\beta_7{}^+$ T and epithelial cells is mediated by the adhesive interaction of $\alpha_E\beta_7$ and E-cadherin; this interaction plays a key role in the damage of target epithelia. To explore the structure-function relationship of the heterophilic adhesive interaction between E-cadherin and $\alpha_E\beta_7$, we performed cell aggregation assays using L cells transfected with an extracellular domain-deletion mutant of E-cadherin. In homophilic adhesion assays, L cells transfected with wild-type or a domain 5-deficient mutant formed aggregates, whereas transfectants with domain 1-, 2-, 3-, or 4-deficient mutants did not. These results indicate that not only domain 1, but domains 2, 3, and 4 are involved in homophilic adhesion. When $\alpha_E\beta_7{}^+$ K562 cells were incubated with L cells expressing the wild type, 23% of the resulting cell aggregates consisted of $\alpha_E\beta_7{}^+$ K562 cells. In contrast, the binding of $\alpha_E\beta_7{}^+$ K562 cells to L cells expressing a domain 5-deficient mutant was significantly decreased, with $\alpha_E\beta_7{}^+$ K562 cells accounting for only 4% of the cell aggregates, while homophilic adhesion was completely preserved. These results suggest that domain 5 is involved in heterophilic adhesion with $\alpha_E\beta_7$, but not in homophilic adhesion, leading to the hypothesis that the fifth domain of E-cadherin may play a critical role in the regulation of heterophilic adhesion to $\alpha_E\beta_7$ and may be a potential target for treatments altering the adhesion of $\alpha_E\beta_7{}^+$ T cells to epithelial cells in inflammatory epithelial diseases. *The Journal of Immunology,* **2005, 175: 1014–1021.**

E-cadherin, a classic member of the cadherin superfamily, is expressed on epithelial cells and mediates Ca^{2+}-dependent homophilic cell-cell adhesion (1–3). Classic cadherins contain five extracellular domains (ECs)[2] of ~110 aa each, a transmembrane domain, and a cytoplasmic domain. Structure-function analyses of the homophilic interactions of E-cadherin have largely focused on the NH_2-terminal EC domain (EC1), which contains a highly conserved His-Ala-Val motif (4–7). Indeed, protein fragments or peptides containing the His-Ala-Val sequence exerted limited effects on cell-cell adhesion (8, 9). Recently, crystallographic analysis has clearly demonstrated that conserved Trp in the EC1 domains of classical cadherins is critical for *trans*-interactions between E-cadherin molecules on different cells, serving as a strand dimer (10). However, several studies have suggested that ECs may be involved in cell adhesion in ways other than the role mediated by EC1. In human cancers, for example, E-cadherin gene mutations frequently occur in exons 7, 8, and/or 9 (corresponding to EC2 and EC3); these mutations are thought to result in the loss of the ability to undergo cell-cell adhesion (11–14). A study on the binding properties of the soluble C-cadherin ectodomain suggested that EC1 was not sufficient for complete homophilic binding (15). Furthermore, Corada et al. (16, 17) demonstrated that mAbs directed against EC3-EC4 affected VE-cadherin adhesion in endothelial cells.

The heterophilic interaction of E-cadherin and integrin $\alpha_E\beta_7$ has been previously documented (18–24). Integrin $\alpha_E\beta_7$ is expressed selectively on intestinal intraepithelial T lymphocytes under physiological conditions (25). Accumulating evidence indicates that $\alpha_E\beta_7{}^+$ is induced on T lymphocytes in the epithelia of skin, lung, salivary, and lacrimal glands and synovial membranes during inflammation (26–31), suggesting that this heterophilic interaction has a pathologic role. Since $\alpha_E\beta_7$ may have an important role in the selective localization or retention of a unique population of T cells in a specific tissue, the adhesion between $\alpha_E\beta_7$ and E-cadherin could be a potential target of therapeutic interventions for epithelial inflammation. Substitutions of a highly exposed and charged amino acid on mouse E-cadherin transfected into L cells demonstrated that Glu^{31} in EC1 is critical for binding with $\alpha_E\beta_7$ (32). Taraszka et al. (33) also elucidated that the substitution of the corresponding Glu in EC1 of human E-cadherin-Fc fusion proteins abrogated binding with $\alpha_E\beta_7$, confirming the previous observations. These studies clearly show that the specific heterophilic adhesion attributed to the exposed Glu^{31} in EC1 differs from homophilic adhesion. With the exception of EC1, however, the structures involved in heterophilic adhesion remain uncertain. To clarify the involvement of the EC domains in both heterophilic and homophilic adhesion, we performed cell aggregation assays using L cells transfected with specific domain-deleted E-cadherin mutations. The present report speculates on the characteristics of the E-cadherin domains involved in homophilic interactions and heterophilic interactions with $\alpha_E\beta_7$.

*Project Research Laboratory, Research Center for Genomic Medicine and †Second Department of Internal Medicine, Saitama Medical Center, Saitama Medical School, Saitama, Japan; and ‡Department of Ophthalmology, Keio University School of Medicine, Tokyo, Japan

Received for publication January 5, 2005. Accepted for publication May 13, 2005.

The costs of publication of this article were defrayed in part by the payment of page charges. This article must therefore be hereby marked *advertisement* in accordance with 18 U.S.C. Section 1734 solely to indicate this fact.

[1] Address correspondence to Dr. Kiyono Shiraishi, Project Research Laboratory, Research Center for Genomic Medicine, Saitama Medical School, 1397-1 Yamane, Hidaka, Saitama 350-1241, Japan. E-mail address: kiyono@saitama-med.ac.jp

[2] Abbreviations used in this paper: EC, extracellular domain; DiO, 3,3′-deoctadecyl-5, 5′-di(4-sulfophenyl)oxacarbocyanine sodium salt.

0022-1767/05/$02.00

Materials and Methods

Cells

Mouse L-K (TK^-) fibroblasts were cultured in DMEM containing 10% FBS. K562 cells were cultured in RPMI 1640 containing 10% FBS. K562 cells double-transfected with α_E and β_7 were a gift from Dr. D. Erle (University of California, San Francisco, CA) and cultured in RPMI 1640 supplemented with 10% FBS, 500 μg/ml hygromycin B, and 500 μg/ml G418 (34).

Construction of E-cadherin deletion mutants

The expression vector containing human E-cadherin cDNA was a gift from Dr. Y. Shimoyama (National Okura Hospital, Tokyo, Japan). To examine the contribution of the different ECs to adhesion, the EC1, EC2, EC3, EC4, or EC5 domains or all of the EC domains were deleted using inverse PCR. Fig. 1 shows the domain deletion mutants (Δ) and the primers designed for the PCR experiments. The following primers were used: for Δ1, 5′-TCTCTTCTGTCTTCTGAGGCCAGGAGAGG-3′ (SIG-R) and 5′-ACCCAGGAGGTCTTTAAGGGGTCTG-3′ (2-F); for Δ2, 5′-GAATTCGGGCTTGTTGTCATTCTG-3′ (1-R) and 5′-AATCCCACCACGTACAGGGTCAG-3′ (3-F); for Δ3, 5′-GAAGATCGGAGGATTATCGTGGT-3′ (2-R) and 5′-GTGCCTCCTGAAAAGAGAGTGGAA-3′ (4-F); for Δ4, 5′-AGGCACAAAGATGGGGGCTTCATTCAC −3′ (3-R) and 5′-GAACCTCGAACTATTCTTCTGT-3′(5-F);forΔ5,5′-TGGTATGGGGGCGTTGTCATTCAC-3′ (4-R) and 5′-ATTCCTGCCATTCTGGGGATTCTTGGAG-3′ (TM-F); and for d0, SIG-R, and TM-F. Amplicons were ligated to form circular plasmids. The structures of the deletion mutants were confirmed by sequencing. Expression vectors bearing wild-type or mutated E-cadherin cDNAs were transfected into L cells using LipofectAMINE reagent (Invitrogen Life Technologies). The transfected cells were selected in DMEM supplemented with 10% FBS and 700 μg/ml G418, and colonies expressing high levels of E-cadherin were screened by Western blot analysis using the mAb 4A2C7 (Zymed).

RT-PCR

One microgram of total RNA from the L transfectants was used to generate single-stranded cDNA using AMV Reverse Transcriptase XL (Takara Bio). The cDNAs were amplified by PCR using Ex *Taq* polymerase (Takara Bio) and the following primers: for EC1, 5′-GACTGGGTTATTCCTCCCATCAGC-3′ (1-F) and 1-R; for EC2, 2-F, and 2-R; for EC3, 3-F, and 3-R; for EC4, 4-F, and 4-R; and for EC5, 5-F, and 5′-TTGCAATCCTGCTTCGACAGGCTGTGC-3′ (5-R).

Western blot

Cultured cells were rinsed in PBS and harvested in mammalian protein extraction reagent (Pierce). The total protein concentration was determined using a Micro BCA protein assay reagent kit (Pierce). GST fusion proteins containing the EC domains were produced in TOP10F′ cells carrying pGEX-4T-2 vectors and purified using GST purification modules (Amersham Biosciences). Cell lysates and the purified fusion proteins were subjected to SDS-PAGE and transferred to an Immobilon-P membrane (Millipore).

The membrane was blocked with 5% skim milk and incubated with the primary Abs. Goat anti-GST Ab was purchased from Amersham Pharmacia. Four different mouse mAbs against human E-cadherin were used. The binding epitopes recognized by SHE78-7 and HECD-1 (Takara Bio) were unknown. 4A2C7 was generated against a recombinant protein corresponding to the cytoplasmic domain, whereas G-10 (Santa Cruz Biotechnology) was raised against a recombinant protein corresponding to aa 600–707. The membrane was then incubated with the respective HRP-conjugated secondary Abs followed by an ECL system (Amersham Biosciences) and analyzed using LAS-1000 (Fuji film).

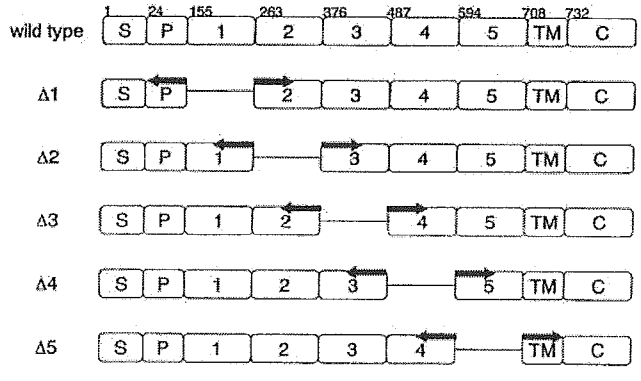

FIGURE 1. Schematic representation of the E-cadherin domain-deletion mutants and the PCR primers. Wild-type E-cadherin has five extracellular cadherin repeats, numbered 1–5 from the NH_2-terminal. The numbers above the columns indicate the amino acid number, counting from the start of the coding region. The arrows represent the primers used for inverse PCR. S, Signal peptide; P, propeptide; TM, transmembrane domain; C, cytoplasmic domain.

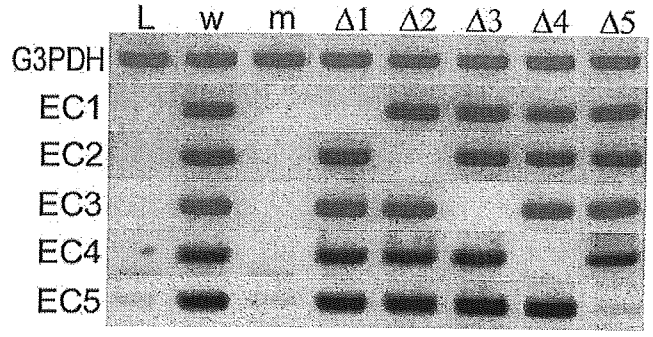

FIGURE 2. Expression of EC mRNA in L cells transfected with E-cadherin domain-deletion mutations. The primers were designed to amplify the various ECs. The mRNAs from parent L cells (L) and L transfectants with wild-type (w), mock (m), and mutated E-cadherin were analyzed using RT-PCR.

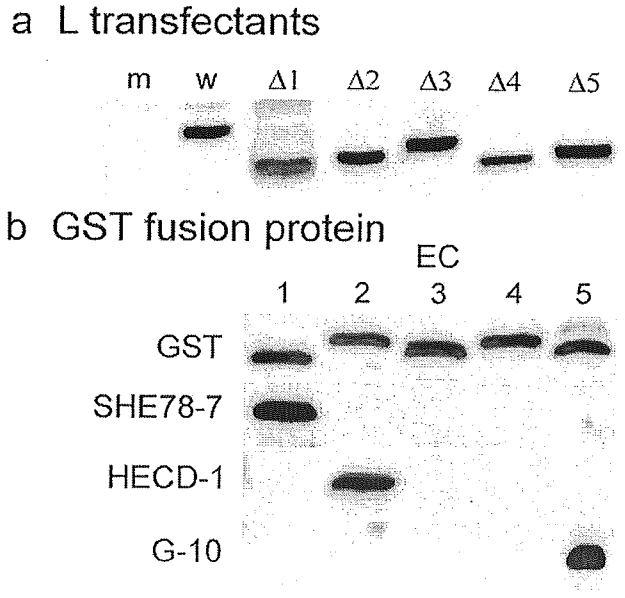

FIGURE 3. *a*, Immunoblot analysis of mutated E-cadherin expression in transfectants. Protein extracts of L cells transfected with mock (m), wild-type (w), and mutated E-cadherin were separated on a 7.5% polyacrylamide gel and transferred to a polyvinylidene difluoride membrane. The membrane was then incubated with anti-E-cadherin Ab 4A2C7, which visualized the 120-kDa band of wild-type E-cadherin. *b*, Identification of the binding epitopes recognized by the mAbs. Purified GST fusion proteins containing the ECs were separated on a 7.5% polyacrylamide gel and transferred to polyvinylidene difluoride membranes. The membranes were incubated with Abs against GST and E-cadherin (SHE78-7, HECD-1, and G-10).

Flow cytometry

The cell surface expression of E-cadherin in the transfectants was examined using flow cytometry. Adherent L transfectants were treated with 0.05% trypsin and 0.02% EDTA at 37°C for 10 min and then washed with DMEM containing 10% FBS. After washing with PBS, the cell suspension was incubated with anti-E-cadherin Ab or an isotype control on ice for 30 min, washed with PBS, and subjected to incubation with FITC-conjugated secondary Ab on ice for 30 min. Ten thousand stained cells were then analyzed using FACSCalibur and the CellQuest software (BD Biosciences).

Cell aggregation assays

The cell aggregation assays were performed according to a method described by Shimoyama et al. (35). Briefly, after the treatment of the adherent cells with 0.05% trypsin and 0.02% EDTA at 37°C for 10 min, the cells were washed and resuspended with DMEM containing 1.8 mM Ca^{2+} and 0.8 mM Mg^{2+} plus 10% FBS. The suspended cells were collected by centrifugation, washed with PBS, and resuspended with the above-mentioned medium.

To examine the homophilic interactions of E-cadherin, 10^5 L transfectants were added to each well of a 24-well plastic plate and incubated with rocking at 37°C overnight in a humidified atmosphere comprised of 7% CO_2 and 93% air. The resulting cell aggregates were examined using a phase-contrast microscope (Olympus).

To examine the heterophilic interactions between E-cadherin and $\alpha_E\beta_7$, L transfectants and K562 transfectants were used in a coaggregation assay. The former transfectants were labeled with 3,3′-dioctadecyl-5, 5′-di(4-sulfophenyl)oxacarbocyanine sodium salt (DiO; Molecular Probes), and the latter were labeled with CellTracker CM-DiI (Molecular Probes). The transfectants were then mixed (5×10^4 cells each), incubated as described above, and observed using a confocal laser-scanning microscope (TCS SP2; Leica). Mg^{2+} (1 mM) was added to the medium when indicated. In some experiments, the proportion of $\alpha_E\beta_7{}^+$ K562 cells in each aggregate was calculated. Micrographs of eight aggregates were taken in each assay. The numbers of K562 and L cells were counted, and the results were expressed as the percentage of K562 cells out of the total number of cells in the aggregate.

In the Ab-blocking experiments, the cells were incubated in the presence of 0.8 μg/ml of appropriate Ab.

Immunocytochemistry

Following the cell aggregation assays, the cell aggregates were collected and washed with PBS. For immunofluorescence staining, the aggregates were incubated with anti-E-cadherin Ab (HECD-1). Subsequently, the samples were incubated with Alexa Fluor 568-conjugated goat anti-mouse IgG Ab (Molecular Probes), followed by incubation with FITC-conjugated anti-$\alpha_E\beta_7$ Ab (Beckman Coulter). The specimens were observed using a confocal laser-scanning microscope.

Results

To confirm whether the transfectants expressed the desired region of E-cadherin, RT-PCR was performed for EC1, EC2, EC3, EC4, and EC5. Fig. 2 shows that the parent L cells did not exhibit any products amplified by human E-cadherin and that all five ECs were expressed in wild-type transfectants. All clones transfected with domain-deletion mutations of E-cadherin exhibited the expected expression patterns: Δ1 lacked EC1, Δ2 lacked EC2, Δ3 lacked EC3, Δ4 lacked EC4, and Δ5 lacked EC5.

The protein expression of mutated E-cadherin was examined by Western blot analysis using the appropriate Abs (Fig. 3*a*). 4A2C7, raised against a recombinant protein corresponding to the cytoplasmic domain, detected all of the deletion mutants. G-10, an alternative E-cadherin Ab that cross-reacts with mouse form (manufacturer's data), could not detect endogenous mouse E-cadherin in mock transfectants (data not shown). To clarify the binding epitopes recognized by the SHE78-7, HECD-1, and G-10 Abs, GST fusion proteins containing the EC domains were analyzed (Fig. 3*b*). SHE78-7 reacted with EC1, whereas HECD-1 reacted with EC2. G-10, raised against a recombinant protein corresponding to EC5, correctly detected EC5.

The expression of the mutated E-cadherin proteins on the cell surfaces of L transfectants was analyzed using flow cytometry (Fig. 4). Approximately 90% of the wild-type and Δ1, Δ3, Δ4, and Δ5 transfectants stained positive when incubated with HECD-1, but the Δ2 transfectants did not. In contrast, the Δ2 transfectants stained positive when incubated with SHE78-7 (Fig. 4); the wild-type, Δ3, Δ4, and Δ5 transfectants also stained positive when incubated with SHE78-7 (data not shown). These results show that the mutated E-cadherin proteins were expressed on the outer cell surface, indicating that protein transport to the plasma membrane was not impaired by the mutations.

To examine the homophilic interactions of the mutated E-cadherin proteins, L transfectants were subjected to a cell aggregation assay (Fig. 5). Mock transfectants were dispersed, whereas L cells expressing wild-type E-cadherin formed closely packed aggregates. Aggregation was strongly inhibited by the addition of SHE78-7 to the assay medium. HECD-1 also inhibited cell aggregation, but its inhibitory effect was not as strong as that of SHE78-7; G-10 did not have any effect on the aggregation. These results indicate that the adhesion of the L cells was mediated through E-cadherin, especially through the EC1 and EC2 domains, but not through the EC5 domain. Higher concentrations of Abs did not influence the results (data not shown).

Next, we examined the interaction of L cells transfected with domain-deletion mutants (Fig. 6). Cell aggregation was completely inhibited not only in the Δ1 transfectants, but also in the Δ2, Δ3, and Δ4 transfectants. In contrast, EC5-deficient transfectants formed cell aggregates. SHE78-7 and HECD-1 Abs also inhibited Δ5 aggregation (Fig. 6, *f* and *g*), indicating that Δ5 aggregates were similar to those produced by wild-type transfectants.

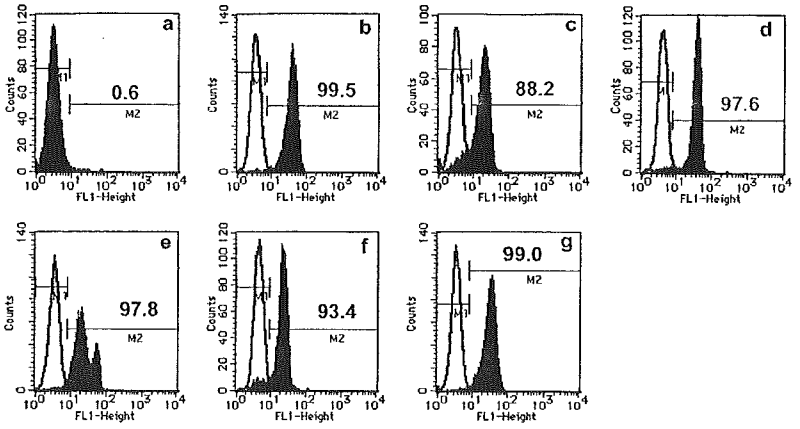

FIGURE 4. Flow cytometry analysis of E-cadherin expression on the cell surface of L transfectants. Mock (*a*), wild-type (*b*), Δ1 (*c*), Δ3 (*e*), Δ4 (*f*), and Δ5 (*g*) transfectants were stained with HECD-1, and Δ2 (*d*) transfectants were stained with SHE78-7. Open histograms indicate background labeling obtained with isotype controls, whereas filled histograms indicate labeling with the Ag-specific Abs.

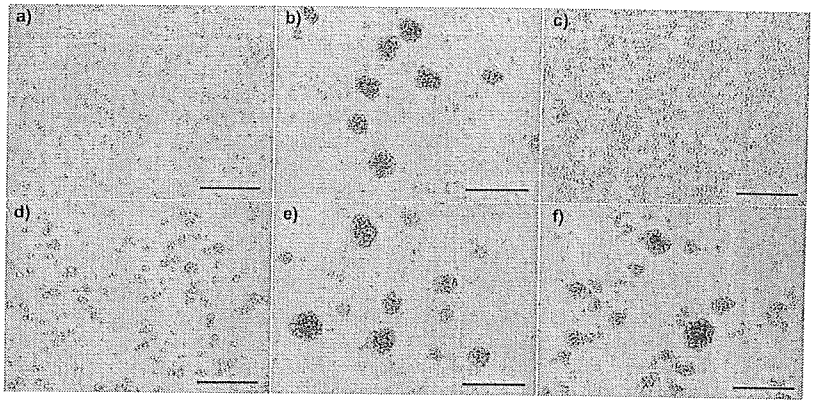

FIGURE 5. Homophilic interaction of wild-type E-cadherin. L cells transfected with mock (*a*) and wild-type (*b*) E-cadherin were used in cell aggregation assays. Wild-type transfectants were incubated in the presence of the anti-E cadherin mAbs SHE78-7 (*c*), HECD-1 (*d*), G-10 (*e*), or an isotype control (*f*). Bars, 300 μm.

To analyze heterophilic interactions, $\alpha_E\beta_7^+$ K562 cells and wild-type E-cadherin$^+$ L cells were mixed. Initially, the $\alpha_E\beta_7^+$ K562 cells did not adhere with the E-cadherin$^+$ L cells; in other words, only the E-cadherin$^+$ L cells adhered and formed cell aggregates (Fig. 7*a*). Thus, we modified the concentration of divalent cations in the assay medium, which originally contained Ca^{2+} and Mg^{2+}. Increasing the Ca^{2+} or Mg^{2+} concentrations had no effect on the aggregate constituents (data not shown). In contrast, Mn^{2+} supplementation led to a number of $\alpha_E\beta_7^+$ K562 cells being included in the cell aggregates (Fig. 7*a*). To confirm this observation, the numbers of the two cell types in each aggregate were counted. As shown in Fig. 8, the percentage of $\alpha_E\beta_7^+$ K562 cells in the cell aggregates significantly increased with Mn^{2+} supplementation (from 5.0 ± 0.8% without Mn^{2+} supplementation to 22.8 ± 0.9% with Mn^{2+} supplementation). Immunofluorescence staining of the cell aggregates clearly showed that E-cadherin and $\alpha_E\beta_7$ were localized on the cell membranes and in close contact (Fig. 7*b*). In subsequent coaggregation assays, Mn^{2+} was added to the assay medium.

The adhesion of $\alpha_E\beta_7^+$ K562 cells to E-cadherin$^+$ L cells was clearly inhibited by the presence of mAb against $\alpha_E\beta_7$, with the percentage of $\alpha_E\beta_7^+$ K562 cells in the cell aggregates decreasing to 2.9 ± 1.1% (Figs. 8 and 9*a*). This result shows that the $\alpha_E\beta_7^+$ K562 cells adhere to the E-cadherin$^+$ L cells via $\alpha_E\beta_7$ during cell aggregation. SHE78-7 inhibited aggregation in the heterophilic assay (Fig. 9*b*), whereas HECD-1 allowed the formation of some aggregates in which $\alpha_E\beta_7^+$ K562 cells were adhered to E-cadherin$^+$ L (23.0 ± 3.1%, Figs. 8 and 9*c*). G-10 did not inhibit the adhesion of the $\alpha_E\beta_7^+$ K562 cells to E-cadherin$^+$ L (25.9 ± 1.2%, Figs. 8 and 9*d*).

Next, the interactions of $\alpha_E\beta_7$ and the mutated E-cadherin proteins were examined. When $\alpha_E\beta_7^+$ K562 cells were mixed with the mock transfectants, no cell aggregates were formed (Fig. 10*a*). Similarly, the Δ1, Δ2, Δ3, or Δ4 transfectants and $\alpha_E\beta_7^+$ K562 cells formed no cell aggregates (data not shown). The mixture of $\alpha_E\beta_7^+$ K562 cells and Δ5 transfectants produced cell aggregates, but the percentage of $\alpha_E\beta_7^+$ K562 cells in the aggregates was significantly lower than that in aggregates formed from the mixture of $\alpha_E\beta_7^+$ K562 cells and wild-type transfectants (4.0 ± 0.9% vs 22.8 ± 0.9%; Figs. 8 and10*b*).

Discussion

In this study, we attempted to clarify the overall binding capability of E-cadherin for both homophilic adhesion and heterophilic adhesion to the integrin $\alpha_E\beta_7$ through the generation of domain-deletion E-cadherin mutants and the transfection of these mutants into L cells to determine the roles of the individual domains in cell adhesion. EC1, EC2, EC3, and EC4 domain-deletion mutants lost their homophilic binding ability, suggesting that these EC domains are indispensable for homophilic adhesion. Substantial evidence

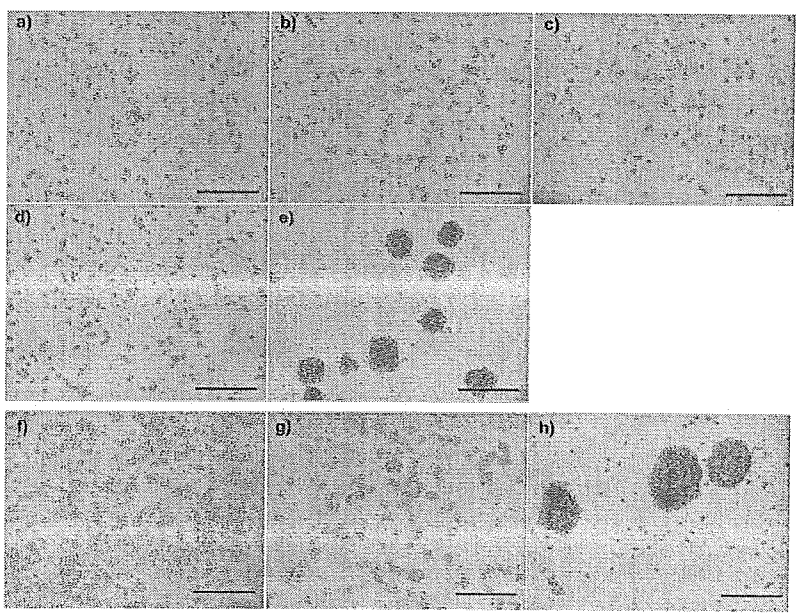

FIGURE 6. Homophilic interactions of domain-deletion mutants. L cells transfected with Δ1 (*a*), Δ2 (*b*), Δ3 (*c*), Δ4 (*d*), and Δ5 (*e*) were used in a cell aggregation assay. Δ5 transfectants were incubated with SHE78-7 (*f*), HECD-1 (*g*), or an isotype control (*h*). Bars, 300 μm.

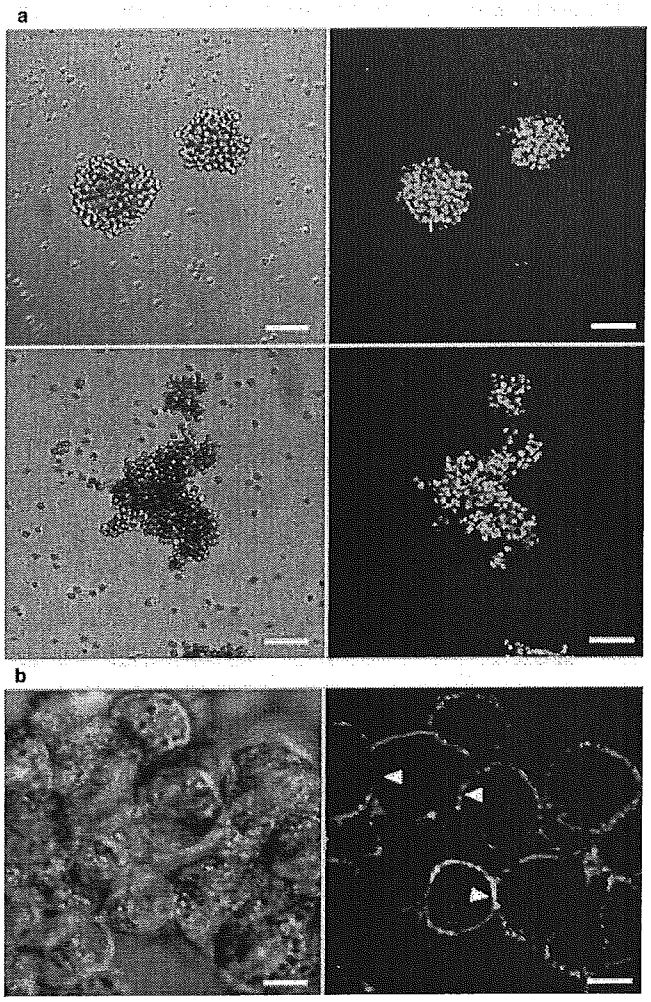

FIGURE 7. *a,* Heterophilic interaction of wild-type E-cadherin with $\alpha_E\beta_7$. Following the labeling of E-cadherin$^+$ L cells with DiO (green) and $\alpha_E\beta_7{}^+$ K562 cells with DiI (red), the cells were allowed to aggregate in assay medium with (*lower*) or without (*upper*) 1 mM Mn^{2+}. The dye localization into cytoplasmic vesicle made DiI-labeled K562 cells look smaller than they really are, while the plasma membrane of L cells was successfully labeled by DiO. Bars, 100 μm. *b,* Immunofluorescence detection of heterophilic aggregates. Cell aggregates were stained with anti-E-cadherin Ab, followed by an Alexa Fluor 568-conjugated secondary Ab, and with FITC-conjugated anti-$\alpha_E\beta_7$ Ab. E-cadherin (red) and $\alpha_E\beta_7$ (green) were localized on the cell membrane and in close contact with each other (arrowheads). Nomarski differential interference micrographs are shown to the *left* of each fluorescent photograph. Bars, 8 μm.

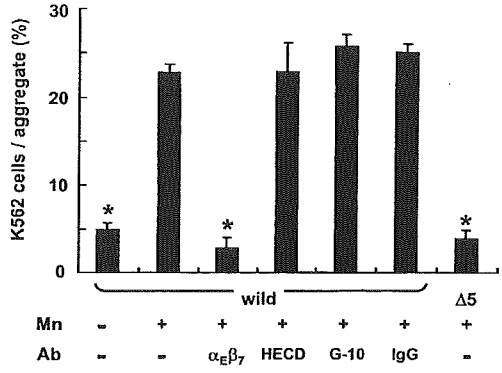

FIGURE 8. Effects of manganese, mAbs, and domain-deletions on heterophilic interactions. The numbers of K562 and L cells were counted, and the results were expressed as the percentage of K562 cells out of the total number of cells in the cell aggregate. Results are shown as the mean ± SEM (n = 8). Student's t test was used for the statistical analysis. The asterisks indicate a significant difference of $p < 0.001$, compared with wild-type transfectants cultured in the presence of Mn^{2+}.

suggests that the combination of *cis*-dimerization of two cadherin molecules on the same cell surface and *trans*-interactions between cadherin dimers on opposing cell surfaces maximizes homophilic adhesion. The widely accepted linear zipper model attributes the adhesive interfaces in the *cis*- and *trans*-interactions to EC1 (6, 7, 36). However, recent studies have introduced a new model for homophilic adhesion. Through the analysis of domain deletions in the *Xenopus* C-cadherin ectodomain using bead aggregation and cell adhesion assays, Clappuis-Flament et al. (15) demonstrated that the combination of at least three EC domains, such as EC1-EC2-EC3 or EC1-EC2-EC4, was required for *trans*-interaction and proposed an alternative model in which multiple ECs are required to achieve full adhesive capability. Several studies have provided data to support this model, suggesting the existence of multiple adhesive interfaces. For example, a mAb recognizing a potential epitope spanning the EC3–EC4 domains affected VE-cadherin adhesion in endothelial cells from umbilical veins (16). A mutant lacking the EC1 domain failed to exhibit homophilic adhesion, although the mutant could adhere to other mutants expressing wild-type E-cadherin (37). In contrast, a crystallographic analysis of C-cadherin supported the linear zipper model by showing that EC1 interacts with EC2 on other E-cadherin molecules on the same cell surface, leading to *cis*-dimerization (10). Our results showing that EC1- or EC2-deficient mutants failed to exhibit full homophilic adhesion are basically consistent with the above findings. However, mutants lacking either the EC3 or EC4 domains also failed to exhibit maximum adhesion. The fact that the present study used mammalian cadherin, whereas the previous study used *Xenopus* cadherin, may partially explain this discrepancy in findings. Another possible explanation may be that intracellular events were affected by the domain deletion in our aggregation assay, since the transmembrane and cytoplasmic domains were included in the domain-deletion human E-cadherin mutants. Compelling evidence suggests that the adhesive strength of cadherin is regulated by the transmembrane and cytoplasmic domains (3, 38–42). For example, the cytoplasmic tail of cadherin interacts with β-catenin and p120, which link cadherin to the actin cytoskeleton through α-catenin, and the regulation of the cadherin-catenin complex by diverse phosphorylation reactions influences the adhesive function of cadherin (43). In addition, the interaction of a motif in domain 4 of N-cadherin with the fibroblast growth factor receptor is required for neurite outgrowth (44), suggesting that EC4 may be involved in a cell signaling pathway in which fibroblast growth factor receptor controls the gene transcription and adhesive activity of cadherin via Snail, resulting in a loss of cell-cell adhesion (43). To the best of our knowledge, little information is available about the involvement of the membrane proximal domain EC5 in homophilic adhesion. EC5 might not participate in the adhesive bond, possibly explaining the preservation of homophilic adhesion in EC5-deficient mutants. Alternatively, conformational changes in E-cadherin resulting from the EC5 deletion may cause cell aggregation via a process different from that occurring with the native molecule. However, current data that the same mAbs inhibiting homotypic aggretgates by wild-type transfectants (SHE78-7, HECD-1) also inhibited those by the Δ5 mutant would be evidence that the process of cell aggregation is similar.

Consistent with previous studies (21, 22, 45), we found that Mn^{2+} stimulated heterophilic interactions between $\alpha_E\beta_7$ and E-cadherin.

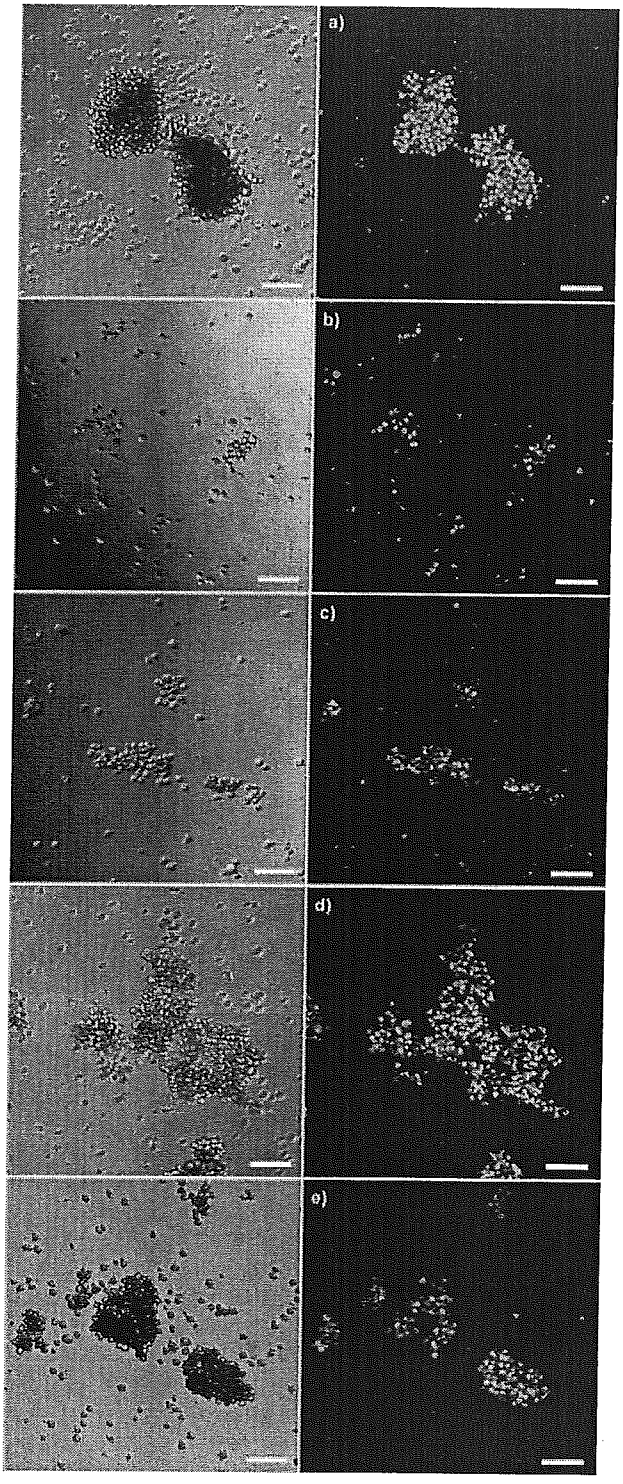

FIGURE 9. Heterophilic interaction of E-cadherin with $\alpha_E\beta_7$. Following the labeling of E-cadherin$^+$ L cells with DiO (green) and $\alpha_E\beta_7{}^+$ K562 cells with DiI (red), the cells were allowed to aggregate in assay medium containing 1 mM Mn^{2+} in the presence of anti-$\alpha_E\beta_7$ Ab (*a*) or one of the anti-E-cadherin Abs SHE78-7 (*b*), HECD-1 (*c*), or G-10 (*d*) or an isotype control (*e*). Nomarski differential interference micrographs are shown to the *left* of each fluorescent photograph. Bars, 100 μm.

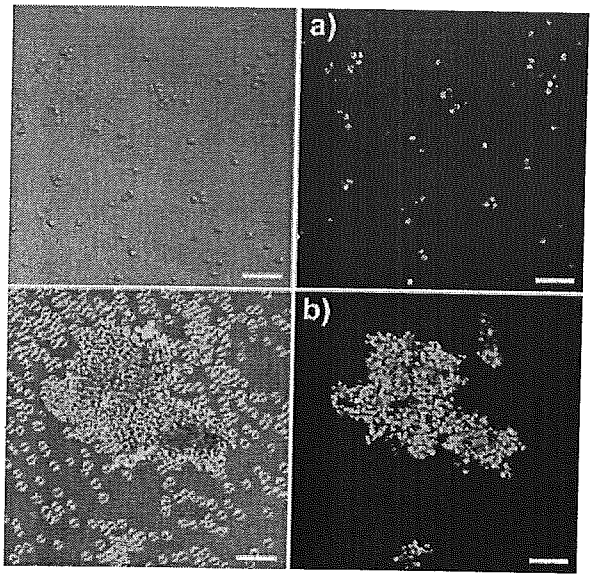

FIGURE 10. Heterophilic interactions of E-cadherin-deletion mutants with $\alpha_E\beta_7$. L cells transfected with mock (*a*) and Δ5 (*b*) were labeled with DiO (green), while the $\alpha_E\beta_7{}^+$ K562 cells were labeled with DiI (red). The cells were allowed to aggregate in assay medium containing 1 mM Mg^{2+}. Nomarski differential interference micrographs are shown to the *left* of each fluorescent photograph. Bars, 100 μm.

The functional activity of integrins is regulated through an inside-out signaling mechanism that quickly switches inactive forms to active forms. Divalent cations are also required for the acquisition of the active state. In particular, manganese has been shown to promote ligand binding by inducing a conformational change in the metal ion-dependent adhesion site (46–48).

To examine homophilic and heterophilic interactions, we adopted a cell aggregation assay that has been frequently used to evaluate cell-cell adhesion activity (4, 15, 35, 37). This assay method produced reproducible and clear results in the present study. When Δ1, Δ2, Δ3, or Δ4 transfectants were mixed with $\alpha_E\beta_7{}^+$ K562 cells, aggregation did not occur, indicating that all four domain-deletion mutants had lost their ability to undergo heterophilic adhesion with $\alpha_E\beta_7$. Alternatively, aggregation may have been prevented by a disruption in homophilic adhesion, although the ability to undergo heterophilic adhesion was retained. Heterophilic interactions have been suggested to be so weak that cell aggregation may not occur without homophilic adhesion; alternatively, $\alpha_E\beta_7$ adhesion may require an E-cadherin homophilic bond to be formed by *trans*-interactions among cells. The mAb HECD-1 against EC2 did not inhibit homophilic aggregation completely, allowing heterophilic adhesion and supporting the possibility that a homophilic scaffold may be necessary for heterophilic interactions. If so, the effect of the Δ1, Δ2, Δ3, and Δ4 mutants cannot be evaluated because these mutants prevent homophilic adhesion, and some degree of homophilic adhesion by the transfected L cells is a prerequisite to allowing a determination of the percentage of K562 cells included in the aggregates of E-cadherin-expressing cells. Therefore, the EC5 deletion mutant is the only mutant of the entire set used in this article that can be evaluated for loss of heterophilic adhesion in the K562 coaggregation assay.

We demonstrated that EC5 is critical for heterophilic adhesion with $\alpha_E\beta_7{}^+$ cells, but not for homophilic adhesion. This is the first evidence showing the involvement of ECs other than EC1 in heterophilic adhesion with $\alpha_E\beta_7$. Since the integrin $\alpha_E\beta_7$ plays a critical role in the selective localization of T cells in inflamed epithelia (26–31, 49), the adhesive interaction could be a potential target for therapeutic interventions. In contrast, mutational analyses of selected residues clearly revealed that the side chain of Glu^{31} is